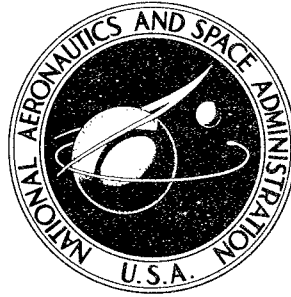


**NASA CONTRACTOR
REPORT**



NASA CR-65

NASA CR-65

56430

DISTRIBUTION STATEMENT A
Approved for Public Release
Distribution Unlimited

PROPERTY OF

**NATURAL FREQUENCIES IN COUPLED
BENDING AND TORSION OF TWISTED
ROTATING AND NONROTATING BLADES**

by G. Isakson and J. G. Eisley

Prepared under Grant No. NsG-27-59 by
UNIVERSITY OF MICHIGAN
Ann Arbor, Michigan
for

20011129 151

NATURAL FREQUENCIES IN COUPLED BENDING AND TORSION
OF TWISTED ROTATING AND NONROTATING BLADES

By G. Isakson and J. G. Easley

Prepared under Grant No. NsG-27-59 by

UNIVERSITY OF MICHIGAN

Ann Arbor, Michigan

This report is reproduced photographically
from copy supplied by the contractor.

NATIONAL AERONAUTICS AND SPACE ADMINISTRATION

For sale by the Office of Technical Services, Department of Commerce
Washington, D. C. 20230 -- Price \$2.25

**Reproduced From
Best Available Copy**

TABLE OF CONTENTS

	Page
LIST OF ILLUSTRATIONS	v
SUMMARY	vii
1. INTRODUCTION	1
2. BLADE ANALYSIS	3
Symbols	3
Basic Matrices	6
Method of Solution	14
Steady-State Deformation	15
Nondimensional Form	18
Numerical Results	27
Discussion of Results	27
3. SIMPLE MODEL ANALYSIS	34
Symbols	34
Description of the Model	36
Derivation of the Equations of Motion	37
Specialization to the Case of Constant Shaft Speed	42
Solution of the Pseudo-Static Problem	46
Formulation and Solution of the Linearized Equations	48
Discussion of Results	50
4. CONCLUDING REMARKS	63
APPENDIX	
A. DIFFERENTIAL EQUATIONS OF MOTION	64
B. RESULTANT LOADINGS	66
C. DEFORMATION OF A BLADE SEGMENT	70
D. CENTRIFUGAL FORCE COUPLING	74
REFERENCES	77

LIST OF ILLUSTRATIONS

TABLE	Page
I. Beam Properties	28
 FIGURE	
2.1. Blade axes.	7
2.2. Nomenclature and sign convention for cross-section coordinates, displacements, bending moments, and shears.	7
2.3. Blade segment rotation.	7
2.4. Effect of twist on natural frequencies of nonrotating blades.	29
2.5. Natural frequencies of rotating blade No. 1.	30
2.6. Natural frequencies of rotating blade No. 2.	31
2.7. Effects of centrifugal force coupling on blade No. 2.	32
3.1. Model coordinates.	37
3.2. Effect of mass offset on pseudo-static displacements of model.	51
3.3. Effect of mass offset on natural vibration characteristics of model.	53
3.4. Effect of mass offset on pseudo-static displacements of model.	54
3.5. Effect of mass offset on natural vibration characteristics of model.	55
3.6. Effect of bending hinge orientation on natural vibration characteristics of model.	56
3.7. Effect of rotational velocity on pseudo-static displacements of model.	57
3.8. Effect of rotational velocity on natural vibration characteristics of model.	58

LIST OF ILLUSTRATIONS (Concluded)

FIGURE	Page
3.9. Response of model as determined by nonlinear and linearized differential equations.	60

SUMMARY

[A Holzer-Myklestad type of procedure, using a matrix formulation, is developed for the determination of the natural vibration characteristics of a pretwisted rotating blade in coupled bending and torsion. The nonrotating blade is considered as a special case. Results of a limited parametric study are presented.] It is found that in the case of the rotating blade there can be an appreciable effect of centrifugal forces in coupling the bending and torsional vibrations.

[In order to investigate the effects of Coriolis forces and the nonlinear effects of large angular displacements, a study is made on the basis of a simple model.] Numerical results indicate that the Coriolis forces may introduce substantial ^{error} phase differences between bending and torsional vibration. Limited numerical results on the nonlinear effects indicate that these effects decrease slightly the frequency of the characteristic motions as determined from a linearized analysis and introduce some coupling between the characteristic motions.

1. INTRODUCTION

In a previous report¹ the natural vibration characteristics of rotating twisted blades were studied for the special case of coincident mass and elastic axes. This eliminates coupling between bending and torsional vibration, and the problem was studied as one in bending vibration only. Bending deformation about both principal axes of the cross section was considered.

The present work represents an extension of this previous work to the case of noncoincident mass and elastic axes, that is, the case of coupled bending and torsion. This case has already been treated analytically in rather complete fashion in Ref. 2, the problem being formulated in terms of governing differential equations and also in terms of energy principles. However, very few results are presented in that reference, and they are for a few special cases of a rather restrictive nature.

In the present work a different analytical approach has been used. It involves essentially an extension of the Holzer-Myklestad method for determining the bending vibrational characteristics of a beam to the case at hand. The Holzer-Myklestad method had previously been extended by Targoff³ to the case of bending of twisted rotating blades and applied in Ref. 1. It was found to be particularly well-suited to automatic digital computation, and, for that reason, has been extended in the present work to include torsion as well, and has been applied in a limited parametric study.

An effect of centrifugal forces in coupling bending and torsional vibration, considered initially in Ref. 2, is taken into account in the present work. It arises when the mass and elastic axes of the blade are not coincident.

It should be remarked that the inclusion of torsional deformation complicates the effects of pretwist and rotation considerably. There may be a sizeable steady-state or "pseudo static" torsional deformation of the rotating blade in some cases. This is due to centrifugal twisting moment which, in the case of negative pretwist and positive pitch, tends to twist the blade negatively, and also to the twisting moment associated with tensile stress in the longitudinal fibers, the so-called "centrifugal untwisting moment." These two effects oppose each other in the normal case, and the extent to which one or the other predominates depends primarily upon the amount of pretwist and the pitch setting of the blade. An analysis of this deformation and presentation of some results are given in Ref. 4.

Additional effects relate to a departure of the torsional stiffness from the value provided by Saint Venant theory. This departure is associated with

inclination of the longitudinal fibers of the blade with respect to the elastic axis, due to both pretwist and torsional deformation. The normal stresses in these fibers can be seen to have components in the plane of a cross section and to exert a torsional moment about the elastic axis. They arise from two sources. Firstly, there are normal stresses associated directly with torsional deformation that are present even in a nonrotating blade. These stresses may introduce a substantial nonlinearity into the torsional stiffness.³⁻⁵ Secondly, there are normal stresses associated with centrifugal forces, contributing to the torsional stiffness in a manner which is essentially linear for practical deformations; that is, there is a linear relationship between torque and elastic twist.^{3,4} Some theoretical results for the case of torsional vibration, with some or all of these effects included, are presented in Refs. 4 and 6.

Because of the possibility of substantial pseudo-static torsional deformation and nonlinearity in the torsional stiffness, an accurate determination of the natural frequencies of vibration of a twisted blade should be based on linearization with respect to the pseudo-static deformation. This has not been done explicitly in generating the results presented in the present report. The values of pretwist selected must be interpreted to include pseudo-static deformation. This facilitates comparison with the results of Ref. 1, where pseudo-static torsional deformation would have an influence on bending vibrational characteristics, and where the values of pretwist must be similarly interpreted to include such deformation.

Another interesting aspect of the rotating blade vibration problem is discussed in Ref. 7. It is shown that Coriolis forces, or so-called "secondary inertia" forces, associated with the combined vibrational and rotational motion introduce a phase difference between the bending and torsional vibration. In order to investigate this effect more fully and to investigate the nonlinear effects of substantial angular displacements on the dynamic characteristics of a rotating blade, an additional study, reported in Section 3, was conducted on the basis of a simple model. The nonlinear effects considered are those associated with inertia forces. Nonlinearity in the torsional stiffness, as discussed above, and the effects of centrifugal tension on the pseudo-static deformation and on torsional stiffness are not included, although they could, in any extension of the present work, be included without undue complication.

2. BLADE ANALYSIS

SYMBOLS

$$A = GJ_e + Tk_A^2 + EB_1(\beta')^2$$

$$\bar{A} = A/EI_{10}$$

B_1, B_2 section constants defined in Appendix A

$$C = EB_2\beta'/A = \bar{C}$$

E Young's modulus

EI_1, EI_2 bending stiffness about major and minor principal centroidal axes, respectively

$$\bar{EI}_1 = EI_1/EI_{10}, \bar{EI}_2 = EI_2/EI_{20}$$

e distance between mass and elastic axis, positive when mass axis lies ahead

$$\bar{e} = e/R$$

e_A distance between area centroid of tensile member and elastic axis, positive when centroid lies ahead

$$\bar{e}_A = e_A/R$$

e_o distance at root between elastic axis and axis about which blade is rotating, positive when elastic axis lies ahead

$$\bar{e}_o = e_o/R$$

GJ_e effective torsional rigidity

$$\bar{GJ}_e = GJ_e/EI_{10}$$

I_ζ, I_η mass moment of inertia of cross section about ζ and η axes, respectively, defined so that corresponding moments for an element dx are $I_\zeta dx$ and $I_\eta dx$

$$\bar{I}_\zeta = I_\zeta/\rho_o R^2 \quad \bar{I}_\eta = I_\eta/\rho_o R^2$$

k_A polar radius of gyration of cross-sectional area effective in carrying tensile stresses about elastic axis

$$\bar{k}_A = k_A/R$$

k_ξ, k_η mass radii of gyration about ξ and η axes, respectively

l length of blade segment

$$\bar{l} = l/R$$

M_1, M_2 bending moment about major and minor principal axes of cross section, respectively, when centrifugal tension is assumed to act along undeformed position of elastic axis

m mass of blade segment

p_x, p_ξ, p_η resultant loadings per unit length in the x, ξ, η directions, respectively

Q resultant torque about elastic axis at any cross section

q_x, q_ξ, q_η resultant torsional loadings per unit length about the x, ξ, η axes, respectively

R blade radius

T centrifugal tension, $\Omega^2 T_1$

$$\bar{T} = \sum_{i=1}^N \bar{\rho}_i \bar{l}_i \bar{x}_i$$

$$T_1 = \sum_{i=1}^N \rho_i l_i x_i$$

u displacement in the x direction

V_1, V_2 shearing forces in the direction of the minor and major principal axes of the cross section, respectively

x, y, z coordinate system which rotates with blade (Fig. 2.2)

$$\bar{x} = x/R$$

$$Y = (EB_2 \beta')^2 / EI_2$$

\bar{Y}	Y/EI_{10}
β	angle between major principal axis of cross section and plane of rotation, either in the undeformed or pseudo-static state
β'	$d\beta/dx$
$\bar{\beta}'$	$\beta'R$
$\Delta\beta$	increment in β between blade segments
γ^2	EI_{10}/EI_{20}
δ_y, δ_z	displacements of the elastic axis in the y and z directions, respectively
δ_1, δ_2	displacements of the elastic axis in the direction of the minor and major principal axes of the cross section, respectively
ζ, η	coordinates in direction of minor and major principal axes, respectively
θ	total twist in blade between $x = 0$ and $x = R$, $\theta = -R\beta'$
λ	$\omega \sqrt{\rho_0 R^4 / EI_{10}}$
μ	$\Omega \sqrt{\rho_0 R^4 / EI_{10}}$
ρ	mass per unit length of blade
$\bar{\rho}$	ρ/ρ_0
ϕ	torsional displacement, positive when leading edge is up
ω	natural frequency of blade vibration
Ω	rotational velocity
[]	rectangular matrix
{ }	column matrix

Other symbols are defined in the text.

Subscripts

n order of natural mode

O value at $x = 0$

T value at $x = R$

()', ()" differentiation with respect to x , except in Appendix C.

BASIC MATRICES

The governing differential equations of motion for a rotating blade with offset mass and elastic axes have been derived and are reported in Ref. 2. These equations are repeated in Appendix A. In the present report these equations have been adapted to a matrix formulation which permits rapid numerical analysis. This method is essentially an extension of the one presented in Ref. 1.

The coordinate axes of the blade are shown in Fig. 2.1. The cross section coordinates and displacements are shown in Fig. 2.2. The blade is divided into a number of spanwise segments, not necessarily equal in length. The mass of each segment is assumed concentrated at its center, and the bending stiffnesses, EI_1 and EI_2 , the torsional stiffness, GJ_e , and the angle of incidence, β , are assumed constant between masses, appropriate average values being selected. The built-in twist is accounted for by relative rotations of adjacent uniform bays (between masses) about a spanwise axis, the change in angle $\Delta\beta$ being equal to the total twist in a segment and occurring just outboard of the mass (Fig. 2.3).

The quantities $V_1, M_1, \delta_1', \delta_1, V_2, M_2, \delta_2', \delta_2, Q$, and ϕ (Fig. 2.2), which apply when the beam is at its maximum displacement in a free vibration, are defined at stations along the beam and may be represented at any station in the form of a column matrix:

$$\{\Delta\} = \left\{ \begin{array}{c} V_1 \\ M_1 \\ \delta_1' \\ \delta_1 \\ V_2 \\ M_2 \\ \delta_2' \\ \delta_2 \\ Q \\ \phi \end{array} \right\} \quad (2.1)$$

The elements of this matrix will vary along the beam in such a manner that the variation can be considered to occur in a series of steps. Moving from the

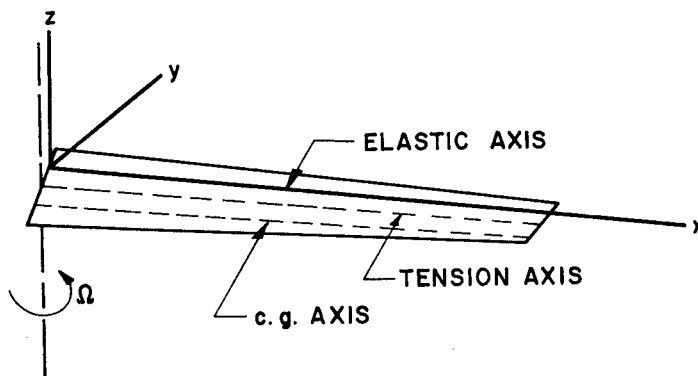


Fig. 2.1. Blade axes.

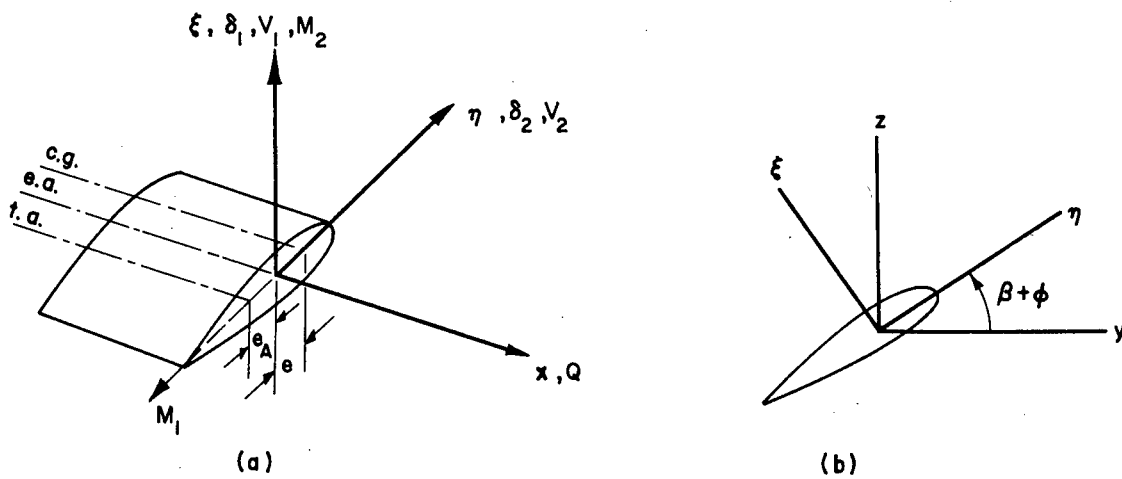


Fig. 2.2. Nomenclature and sign convention for cross-section coordinates, displacements, bending moments, and shears.

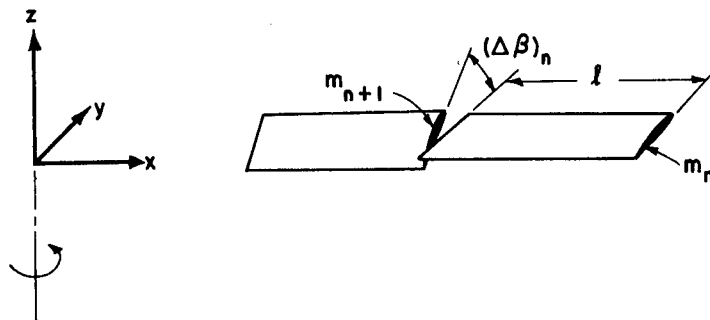


Fig. 2.3. Blade segment rotation.

tip toward the root of the beam, the change in $\{\Delta\}$ occurring from a station immediately outboard of one mass to a station immediately outboard of the next mass can be broken down into three steps, the first involving movement across the mass, the second involving movement from one end to the other of a weightless uniform bay, and the third involving movement across the discontinuity in β .

The relationship between the $\{\Delta\}$ matrices as they apply at the two extremes of this travel can be represented as follows:

$$\{\Delta\}_{n+1} = [R][E][F]\{\Delta\}_n \quad (2.2)$$

where $[F]$, $[E]$, and $[R]$ are rectangular matrices representing linear relationships corresponding to the three steps discussed previously.

The $[F]$ matrix, relating the $\{\Delta\}$ matrices on either side of a concentrated mass, is written as follows:

$$F = \begin{bmatrix} 1 & 0 & 0 & F_{14} & 0 & 0 & 0 & F_{18} & 0 & F_{110} \\ 0 & 1 & F_{23} & F_{24} & 0 & 0 & 0 & 0 & 0 & 0 \\ 0 & 0 & 1 & 0 & 0 & 0 & 0 & 0 & 0 & 0 \\ 0 & 0 & 0 & 1 & 0 & 0 & 0 & 0 & 0 & 0 \\ 0 & 0 & 0 & F_{54} & 1 & 0 & 0 & F_{58} & 0 & F_{510} \\ 0 & 0 & 0 & 0 & 0 & 1 & F_{67} & F_{68} & 0 & 0 \\ 0 & 0 & 0 & 0 & 0 & 0 & 1 & 0 & 0 & 0 \\ 0 & 0 & 0 & 0 & 0 & 0 & 0 & 1 & 0 & 0 \\ 0 & 0 & 0 & F_{94} & 0 & 0 & 0 & F_{98} & 1 & F_{910} \\ 0 & 0 & 0 & 0 & 0 & 0 & 0 & 0 & 0 & 1 \end{bmatrix} \quad (2.3)$$

where

$$\begin{aligned} F_{14} &= l\rho(\omega^2 + \Omega^2 \sin^2 \beta) \\ F_{18} &= -l\rho\Omega^2 \sin \beta \cos \beta \\ F_{110} &= l\rho e\{\omega^2 + \Omega^2(\sin^2 \beta - \cos^2 \beta)\} - l\rho e_0 \Omega^2 \cos \beta \\ F_{23} &= \frac{\rho l^3 \omega^2}{12} + lI_\eta(\omega^2 + \Omega^2) \end{aligned} \quad (2.4)$$

$$\begin{aligned}
F_{24} &= -\rho l x \Omega^2 \\
F_{210} &= -\rho l e x \Omega^2 \\
F_{54} &= F_{18} \\
F_{58} &= \rho l (\omega^2 + \Omega^2 \cos^2 \beta) \\
F_{510} &= -2\rho l e \Omega^2 \sin \beta \cos \beta - \rho l \Omega^2 e_0 \sin \beta \\
F_{67} &= \frac{\rho l^3 \omega^2}{12} + l I_\zeta (\omega^2 + \Omega^2) \\
F_{68} &= F_{24} \\
F_{94} &= \rho l e (\omega^2 + \Omega^2 \sin^2 \beta) \\
F_{98} &= -\rho l e \Omega^2 \sin \beta \cos \beta \\
F_{910} &= l (I_\zeta + I_\eta) \omega^2 + (I_\eta - I_\zeta) (\cos^2 \beta - \sin^2 \beta) l \Omega^2 - l \rho e e_0 \Omega^2 \cos \beta \quad (2.4)
\end{aligned}$$

The derivation of the elements of this matrix is given in detail in Appendix B, except for the contribution of centrifugal force coupling, which is treated separately in Appendix D. It is seen that only the shear forces, bending moments, and torque are changed, since there are no discontinuities in slope or displacement. The changes in shear force are due partly to the inertia force associated with the vibrational motion of the mass and partly to the component of centrifugal force normal to the undeformed position of the elastic axis. Part of the change in torque is related to the change in shear, since the mass and elastic axes do not coincide, and part is due to the inertia force associated with the torsional vibrational motion. The change in bending moment, except that associated with centrifugal force coupling, is fictitious and arises from a special feature of the analysis. This feature involves the replacement of the component of the centrifugal force parallel to the undeformed position of the elastic axis by an equal force along the line of the undeformed axis and an appropriate couple to provide static equivalence. The changes in bending moment indicated in the [F] matrix are then due only to the applied couple, the moment due to the force applied along the undeformed axis being accounted for in the [E] matrix. When moments due to both sources are considered, the discontinuity in bending moment disappears. Note that, on the basis of this procedure, the bending moment at any station is not M, but rather M plus the moment of the tensile force T acting along the undeformed elastic axis.

The elements in the [E] matrix are found by the solution of the differential equations of combined bending and torsion of the weightless uniform bay between masses. These equations and their solutions are given in Appen-

dix C. The resulting [E] matrix is:

$$E = \begin{bmatrix} 1 & 0 & 0 & 0 & 0 & 0 & 0 & 0 & 0 & 0 \\ E_{21} & 1 & 0 & 0 & 0 & 0 & 0 & 0 & 0 & 0 \\ E_{31} & E_{32} & E_{33} & E_{34} & E_{35} & E_{36} & E_{37} & E_{38} & E_{39} & E_{310} \\ E_{41} & E_{42} & E_{43} & E_{44} & E_{45} & E_{46} & E_{47} & E_{48} & E_{49} & E_{410} \\ 0 & 0 & 0 & 0 & 1 & 0 & 0 & 0 & 0 & 0 \\ 0 & 0 & 0 & 0 & E_{65} & 1 & 0 & 0 & 0 & 0 \\ E_{71} & E_{72} & E_{73} & E_{74} & E_{75} & E_{76} & E_{77} & E_{78} & E_{79} & 0 \\ E_{81} & E_{82} & E_{83} & E_{84} & E_{85} & E_{86} & E_{87} & E_{88} & E_{89} & 0 \\ 0 & 0 & 0 & 0 & 0 & 0 & 0 & 0 & 1 & 0 \\ E_{101} & E_{102} & E_{103} & E_{104} & E_{105} & E_{106} & E_{107} & E_{108} & E_{109} & E_{1010} \end{bmatrix} \quad (2.5)$$

where, if we define

$$\begin{aligned} P_1 &= \frac{(p_1^2 - a_1)(p_2^2 - a_1)}{(a_1 - a_3)(p_1^2 - p_2^2)} \\ P_2 &= \frac{(p_1^2 - a_1)(p_2^2 - a_3)}{(a_1 - a_3)(p_1 - p_2)} \\ P_3 &= \frac{(p_1^2 - a_3)(p_2^2 - a_1)}{(a_1 - a_3)(p_1^2 - p_2^2)} \\ P_4 &= \frac{(p_1^2 - a_3)(p_2^2 - a_3)}{(a_1 - a_3)(p_1^2 - p_2^2)} \end{aligned} \quad (2.6)$$

the components of E are given below. The quantities p_i , a_i , and f_i are defined in Appendix C.

$$E_{21} = l$$

$$E_{31} = -\frac{1}{f_2 EI_1} \left\{ (a_2 a_6 P_4 - a_3 a_8 P_3) \cosh p_1 l + [-a_2 a_6 P_4 + a_3 a_8 (P_3 + 1)] \cosh p_2 l - a_3 a_8 \right\}$$

$$E_{32} = + \frac{P_3}{EI_1 p_1} \sinh p_1 l + \frac{P_2}{EI_1 p_2} \sinh p_2 l \quad (2.7)$$

$$E_{33} = - P_3 \cosh p_1 l + P_2 \cosh p_2 l$$

$$E_{34} = -a_1 EI_1 E_{32}$$

$$E_{35} = -\frac{a_2 P_4}{a_3 a_4 EI_2} \left(\frac{1}{p_1} \sinh p_1 l - \frac{1}{p_2} \sinh p_2 l \right)$$

$$E_{36} = -\frac{a_2 P_4}{a_3 a_4 EI_2} (\cosh p_1 l - \cosh p_2 l)$$

$$E_{37} = a_3 EI_2 E_{35}$$

$$E_{38} = -a_3 EI_2 E_{36}$$

$$E_{39} = -\frac{a_2}{f_2(p_1^2 - p_2^2)} \left[-(p_1^2 - a_3)p_2^2 \cosh p_1 l + (p_2^2 - a_3)p_1^2 \cosh p_2 l \right] + \frac{a_2 a_3}{f_2}$$

$$E_{310} = -a_2 EI_1 E_{32} + E_{36} W^{(N)}$$

$$E_{41} = \frac{1}{f_2 EI_1} \left\{ (-a_3 a_8 P_3 + a_2 a_8 P_4) \frac{1}{p_1} \sinh p_1 l + [a_3 a_8 (P_3 + 1) - a_2 a_8 P_4] \frac{1}{p_2} \sinh p_2 l - a_3 a_8 l \right\} \quad (2.7)$$

$$E_{42} = \frac{1}{EI_1} \left[\frac{-p_1^2 (p_2^2 - a_3) + a_3 (p_2^2 - a_1)}{(a_1 - a_3) p_1 p_2^2} - \frac{P_3}{p_1} \cosh p_1 l + \frac{P_2}{p_2} \cosh p_2 l \right]$$

$$E_{43} = -EI_1 E_{32}$$

$$E_{44} = -\frac{a_3 (p_1^2 - p_2^2) P_1}{p_1 p_2^2} - \frac{a_1 P_3}{p_1^2} \cosh p_1 l + \frac{a_1 P_2}{p_2^2} \cosh p_2 l$$

$$E_{45} = \frac{a_2 P_4}{a_3 a_4 p_1 p_2^2 EI_2} \left[(p_1^2 - p_2^2) + p_2^2 \cosh p_1 l - p_1^2 \cosh p_2 l \right]$$

$$E_{46} = E_{35}$$

$$E_{47} = -a_3 EI_2 E_{45}$$

$$E_{48} = E_{37}$$

$$E_{49} = \frac{a_2}{f_2(p_1^2 - p_2^2)} \left[-(p_1^2 - a_3) \frac{p_2^2}{p_1} \sinh p_1 l + (p_2^2 - a_3) \frac{p_1^2}{p_2} \sinh p_2 l \right] + \frac{a_2 a_3 l}{f_2}$$

$$E_{410} = a_2 EI_1 E_{42} + E_{46} W^{(N)}$$

$$E_{65} = l$$

$$E_{71} = -\frac{a_4}{a_2 f_2 EI_1} \left[(a_2 a_6 P_2 - a_3 a_8 P_1) p_1 \sinh p_1 l + (-a_2 a_6 P_3 + a_3 a_8 P_1) p_2 \sinh p_2 l \right]$$

$$E_{72} = + \frac{a_4 P_1}{a_2 EI_1} (\cosh p_1 l - \cosh p_2 l)$$

$$E_{73} = \frac{a_4 P_1}{a_2} (-p_1 \sinh p_1 l + p_2 \sinh p_2 l)$$

$$E_{74} = -a_1 EI_1 E_{72}$$

$$E_{75} = -\frac{1}{a_3 EI_2} (E_{77} - 1)$$

(2.7)

$$E_{76} = -\frac{1}{a_3 EI_2} (P_2 p_1 \sinh p_1 l - P_3 p_2 \sinh p_2 l)$$

$$E_{77} = P_2 \cosh p_1 l - P_3 \cosh p_2 l$$

$$E_{78} = -a_3 EI_2 E_{76}$$

$$E_{79} = -\frac{a_4 P_1 P_2}{f_2(p_1^2 - p_2^2)} \left[-(p_1^2 - a_1) \frac{\sinh p_1 l}{p_2} + (p_2^2 - a_1) \frac{\sinh p_2 l}{p_1} \right]$$

$$E_{710} = -a_2 EI_1 E_{72} + E_{76} W^{(N)}$$

$$E_{81} = \frac{a_4}{a_2 f_2 EI_1} \left[(a_2 a_6 P_2 - a_3 a_8 P_1) \cosh p_1 l + (-a_2 a_6 P_3 + a_3 a_8 P_1) \cosh p_2 l - a_2 a_6 \right]$$

$$E_{82} = -\frac{a_4 P_1}{a_2 EI_1} \left(\frac{1}{p_1} \sinh p_1 l - \frac{1}{p_2} \sinh p_2 l \right)$$

$$E_{83} = -EI_1 E_{72}$$

$$E_{84} = a_1 EI_1 E_{82}$$

$$E_{85} = \frac{1}{a_3 EI_2} (E_{87} - l)$$

$$E_{86} = \frac{1}{a_3 EI_2} (E_{88} - l)$$

$$E_{87} = -\frac{P_2}{p_1} \sinh p_1 l + \frac{P_3}{p_2} \sinh p_2 l$$

$$E_{88} = P_2 \cosh p_1 l - P_3 \cosh p_2 l$$

$$E_{89} = \frac{a_4}{f_2(p_1^2 - p_2^2)} \left[-(p_1^2 - a_1)p_2^2 \cosh p_1 l + (p_2^2 - a_1)p_1^2 \cosh p_2 l \right] + \frac{a_1 a_4}{f_2}$$

$$E_{810} = a_2 EI_1 E_{82} + E_{86} W^{(N)}$$

$$E_{101} = \frac{1}{a_2 f_2 EI_1} \left[\frac{(p_1^2 - a_3)}{p_1} (a_2 a_6 P_2 - a_3 a_8 P_1) \sinh p_1 l \right. \\ \left. - \frac{(p_2^2 - a_3)}{p_2} (a_2 a_6 P_3 - a_3 a_8 P_1) \sinh p_2 l + a_2 a_3 a_6 l \right]$$

(2.7)

$$E_{102} = \frac{P_1}{a_2 p_1 p_2^2 EI_1} \left[a_3 (p_1^2 - p_2^2) - (p_1^2 - a_3)p_2^2 \cosh p_1 l + (p_2^2 - a_3)p_1^2 \cosh p_2 l \right]$$

$$E_{103} = -\frac{P_1}{a_2} \left[-\frac{(p_1^2 - a_3)}{p_1} \sinh p_1 l + \frac{(p_2^2 - a_3)}{p_2} \sinh p_2 l \right]$$

$$E_{104} = a_1 EI_1 E_{102}$$

$$E_{105} = \frac{P_4}{a_3 a_4 p_1^2 p_2^2 EI_2} \left[-a_1 (p_1^2 - p_2^2) + (p_1^2 - a_1)p_2^2 \cosh p_1 l - (p_2^2 - a_1)p_1^2 \cosh p_2 l \right]$$

$$E_{106} = \frac{P_4}{a_3 a_4 EI_2} \left[\frac{(p_1^2 - a_1)}{p_1} \sinh p_1 l - \frac{(p_2^2 - a_1)}{p_2} \sinh p_2 l \right]$$

$$E_{107} = -a_3 EI_2 E_{105}$$

$$E_{108} = a_3 EI_2 E_{106}$$

$$\begin{aligned}
E_{109} &= \frac{1}{f_2} \left[-a_1 a_3 l - \frac{(p_1^2 - a_1)(p_1^2 - a_3)p_2^2}{(p_1^2 - p_2^2)p_1} \sinh p_1 l + \frac{(p_2^2 - a_1)(p_2^2 - a_3)p_1^2}{(p_1^2 - p_2^2)p_2} \sinh p_2 l \right] \\
E_{1010} &= \frac{1}{p_1 p_2^2} \left\{ \frac{a_1}{(a_1 - a_3)} \left[p_1^2 (p_2^2 - a_3) - a_3 (p_2^2 - a_1) \right] + P_1 \left[-(p_1^2 - a_3) p_2^2 \cosh p_1 l \right. \right. \\
&\quad \left. \left. + (p_2^2 - a_3) p_1^2 \cosh p_2 l \right] \right\} + E_{106} W^{(N)} \quad (2.7)
\end{aligned}$$

Note that δ_1' and δ_2' are positive for increasing deflection in the positive x direction.

The [R] matrix serves to rotate the coordinate axes through the angle $\Delta\beta$ and is written as follows:

$$[R] = \begin{bmatrix} \cos \Delta\beta & 0 & 0 & 0 & -\sin \Delta\beta & 0 & 0 & 0 & 0 & 0 \\ 0 & \cos \Delta\beta & 0 & 0 & 0 & -\sin \Delta\beta & 0 & 0 & 0 & 0 \\ 0 & 0 & \cos \Delta\beta & 0 & 0 & 0 & -\sin \Delta\beta & 0 & 0 & 0 \\ 0 & 0 & 0 & \cos \Delta\beta & 0 & 0 & 0 & -\sin \Delta\beta & 0 & 0 \\ \sin \Delta\beta & 0 & 0 & 0 & \cos \Delta\beta & 0 & 0 & 0 & 0 & 0 \\ 0 & \sin \Delta\beta & 0 & 0 & 0 & \cos \Delta\beta & 0 & 0 & 0 & 0 \\ 0 & 0 & \sin \Delta\beta & 0 & 0 & 0 & \cos \Delta\beta & 0 & 0 & 0 \\ 0 & 0 & 0 & \sin \Delta\beta & 0 & 0 & 0 & \cos \Delta\beta & 0 & 0 \\ 0 & 0 & 0 & 0 & 0 & 0 & 0 & 0 & 1 & 0 \\ 0 & 0 & 0 & 0 & 0 & 0 & 0 & 0 & 0 & 1 \end{bmatrix} \quad (2.8)$$

METHOD OF SOLUTION

By a successive multiplication of the appropriate matrices, a linear relationship can be established between the $\{\Delta\}$ matrices at the root and tip of the beam

$$\{\Delta\}_{\text{root}} = [C]\{\Delta\}_{\text{tip}} \quad (2.9)$$

Recognizing that the shears, bending moments, and torque are zero at the tip of the beam, the $\{\Delta\}_{\text{tip}}$ matrix can be reduced to a five-element matrix, and the corresponding five columns can be eliminated from the first [F] matrix at the tip of the beam; successive multiplications will then yield a 10 x 5 matrix product.

In order to satisfy the boundary conditions at the root of the beam, the determinant of a 5 x 5 matrix formed from appropriate elements of the [C] matrix must equal zero. For example, for a cantilever blade the third, fourth,

seventh, eighth, and tenth rows form the 5 x 5 determinant, and for a fully articulated blade with torsional restraint the second, fourth, sixth, eighth, and tenth rows form the determinant. Other boundary conditions, such as elastic restraint at the root, can be handled easily.

The elements of this determinant will be polynomials in ω^2 , and upon expansion a polynomial equation in ω^2 will be obtained. In principle, the natural frequencies of the blade could be determined by solving for the roots of this equation; however, such a procedure is far too cumbersome to be feasible.

A more practical procedure involves the introduction of trial values of ω into the various $[F]$ matrices and evaluating the elements of all matrices numerically. The matrix multiplications can then be carried out numerically, and the appropriate determinant evaluated. The value of this determinant, which may be termed the "residual," may then be plotted versus ω or ω^2 and the location of the zeros of the residual will determine the natural frequencies of the blade.

STEADY-STATE DEFORMATION

As pointed out in the introduction, there may be a sizable steady-state or "pseudo-static" torsional deformation of the rotating blade in some cases. The loadings which produce this deformation are given in Appendix B along with those induced by the lateral and torsional vibratory motion. It is possible to determine this pseudo-static deformation and to then find the natural frequencies based on linearization with respect to the pseudo-static deformation. In the numerical results which follow this has not been done explicitly. The values of pretwist selected should be interpreted to include the pseudo-static deformation.

In order to determine the pseudo-static deformation let us define the following matrices:

$\{\Delta\}_i$ = column matrix of blade variables just outboard of mass i

$\{\hat{\Delta}\}_i$ = column matrix of blade variables just inboard of mass i

$[F_0]_i$ = matrix $[F]$ with $\omega = 0$, across mass i

$\{d\}_i$ = column matrix of steady state quantities across mass i

$\{g\}_i$ = column matrix of steady state quantities across bay between masses i and $i+1$

$[D]_i$ = $[R]_i [E]_i$ across bay between masses i and $i+1$.

Then it follows that

$$\left\{ \begin{bmatrix} \hat{\Delta}_i \\ -1 \end{bmatrix} \right\} = \begin{bmatrix} [F_o]_i & \{d\}_i \\ [O] & -1 \end{bmatrix} \left\{ \begin{bmatrix} \Delta_i \\ -1 \end{bmatrix} \right\} \quad (2.10)$$

and

$$\left\{ \begin{bmatrix} \Delta_{i+1} \\ -1 \end{bmatrix} \right\} = \begin{bmatrix} [D]_i & \{g\}_i \\ [O] & -1 \end{bmatrix} \left\{ \begin{bmatrix} \hat{\Delta}_i \\ -1 \end{bmatrix} \right\} \quad (2.11)$$

Starting at the root where

$$\{\Delta\}_{\text{root}} = \{\Delta\}_{n+1} \quad ,$$

we have

$$\left\{ \begin{bmatrix} \Delta_{\text{root}} \\ -1 \end{bmatrix} \right\} = \begin{bmatrix} [H] & \{h\} \\ [O] & -1 \end{bmatrix} \left\{ \begin{bmatrix} \Delta_1 \\ -1 \end{bmatrix} \right\} \quad , \quad (2.12)$$

where

$$\begin{bmatrix} [H] & \{h\} \\ [O] & -1 \end{bmatrix} = \prod_{i=1}^n \begin{bmatrix} [D]_i & \{g\}_i \\ [O] & -1 \end{bmatrix} \begin{bmatrix} [F_o]_i & \{d\}_i \\ [O] & -1 \end{bmatrix}$$

and in which i decreases as one proceeds from left to right.
Equation (2.12) may be written

$$\{\Delta\}_{\text{root}} = [H]\{\Delta\}_1 + \{h\} \quad . \quad (2.12a)$$

Satisfying the boundary conditions at the root and the tip of the blade, Eq. (2.12) may be reduced to

$$[H^{(K)}] \{\Delta^{(1)}\}_1 = -\{h^{(K)}\} \quad , \quad (2.13)$$

where

$$\{\Delta^{(1)}\} = \begin{Bmatrix} \delta_1 \\ \delta_1 \\ \delta_2 \\ \delta_2 \\ \phi \end{Bmatrix} \quad (2.14)$$

and where $K = 1$ corresponds to a fixed root, and $K = 2$ corresponds to a fully articulated root ($M_1 = M_2 = 0$). $[H^{(K)}]$ is a square matrix of order 5, and $\{h^{(K)}\}$ is a five element column matrix.

In the case of a fixed root, $[H^{(1)}]$ is obtained by deleting rows 1, 2, 5, 6, and 9 and columns 1, 2, 5, 6, and 9 from $[H]$, and $\{h^{(1)}\}$ is obtained by deleting rows 1, 2, 5, 6, and 9 from $\{h\}$. Similarly, in the case of a fully articulated blade, $[H^{(2)}]$ is obtained by deleting rows 1, 3, 5, 7, 9 and columns 1, 2, 5, 6, and 9 from $[H]$, and $\{h^{(2)}\}$ is obtained by deleting rows 1, 3, 5, 7, and 9 from $\{h\}$.

Equation (2.13) may be solved for $\{\Delta^{(1)}\}$, and $\{\Delta\}$ then determined for all stations by applying Eqs.(2.10) and (2.11), starting at the tip and progressing toward the root.

The matrices $\{d\}$ and $\{g\}$ are each ten-element column matrices which are obtained from the steady state terms in Appendices B and C. From Appendix B,

$$\begin{aligned} d_1 &= -\rho l \Omega^2 \sin \beta (e_0 + e \cos \beta) \\ d_2 &= d_3 = d_4 = d_7 = d_8 = d_{10} = 0 \\ d_5 &= \rho l \Omega^2 \cos \beta (e_0 + e \cos \beta) \\ d_6 &= -\rho l \times e \Omega^2 \\ d_9 &= (I_\eta - I_\xi) \Omega^2 \sin \beta \cos \beta - \rho l e e_0 \Omega^2 \sin \beta \end{aligned} \quad (2.15)$$

Appendix C shows that the $\{g\}$ matrix can be derived from the $[E]$ matrix if the terms involving M_2 and Q are extracted and M_2 and Q are replaced by Te_A and $Tk_A^z \beta'$, respectively. Thus,

$$g_i = E_{i2} Te_A + E_{i9} Tk_A^z \beta' \quad (2.16)$$

NONDIMENSIONAL FORM

It is convenient and desirable to treat the problem in nondimensional form. The $\{\Delta\}$ matrix can be redefined in terms of nondimensional forces, moments, and deformations as follows:

$$\{\bar{\Delta}\} = \left\{ \begin{array}{c} V_1 R^2 / EI_{10} \\ M_1 R / EI_{10} \\ \delta_1' \\ \delta_1 / R \\ V_2 R^2 / EI_{10} \\ M_2 R / EI_{10} \\ \delta_2' \\ \delta_2 / R \\ QR / EI_{10} \\ \phi \end{array} \right\} \quad (2.17)$$

The corresponding nondimensional form for the $[F]$ matrix follows:

$$[\bar{F}] = \begin{bmatrix} 1 & 0 & 0 & \bar{F}_{14} & 0 & 0 & 0 & \bar{F}_{18} & 0 & \bar{F}_{110} \\ 0 & 1 & \bar{F}_{23} & \bar{F}_{24} & 0 & 0 & 0 & 0 & 0 & 0 \\ 0 & 0 & 1 & 0 & 0 & 0 & 0 & 0 & 0 & 0 \\ 0 & 0 & 1 & 0 & 0 & 0 & 0 & 0 & 0 & 0 \\ 0 & 0 & 0 & \bar{F}_{54} & 1 & 0 & 0 & \bar{F}_{58} & 0 & \bar{F}_{510} \\ 0 & 0 & 0 & 0 & 0 & 1 & \bar{F}_{67} & \bar{F}_{68} & 0 & 0 \\ 0 & 0 & 0 & 0 & 0 & 0 & 1 & 0 & 0 & 0 \\ 0 & 0 & 0 & 0 & 0 & 0 & 0 & 1 & 0 & 0 \\ 0 & 0 & 0 & \bar{F}_{94} & 0 & 0 & 0 & \bar{F}_{98} & 1 & \bar{F}_{910} \\ 0 & 0 & 0 & 0 & 0 & 0 & 0 & 0 & 0 & 1 \end{bmatrix} \quad (2.18)$$

where

$$\bar{F}_{14} = \bar{l}\bar{\rho}(\lambda^2 + \mu^2 \sin^2 \beta)$$

$$\bar{F}_{18} = -\bar{l}\bar{\rho}\mu^2 \sin \beta \cos \beta$$

$$\bar{F}_{110} = \bar{\rho}\bar{l}\bar{e}(\lambda^2 + \mu^2 (\sin^2 \beta - \cos^2 \beta)) - \bar{\rho}\bar{l}\bar{e}_0\mu^2 \cos \beta$$

$$\bar{F}_{23} = \frac{\bar{\rho}\bar{l}^3\lambda^2}{12} + \bar{l}\bar{I}_\eta(\lambda^2 + \mu^2)$$

$$\bar{F}_{24} = -\bar{\rho}\bar{l}\bar{x}\mu^2$$

$$\bar{F}_{210} = -\mu^2\bar{\rho}\bar{l}\bar{e}\bar{x}$$

$$\bar{F}_{54} = \bar{F}_{18}$$

(2.19)

$$\bar{F}_{58} = \bar{\rho}\bar{l}(\lambda^2 + \mu^2 \cos^2 \beta)$$

$$\bar{F}_{510} = -\bar{\rho}\bar{l}\mu^2 \sin \beta (2\bar{e} \cos \beta + \bar{e}_0)$$

$$\bar{F}_{67} = \frac{\bar{\rho}\bar{l}^3\lambda^2}{12} + \bar{l}\bar{I}_\zeta(\lambda^2 + \mu^2)$$

$$\bar{F}_{68} = \bar{F}_{24}$$

$$\bar{F}_{94} = \bar{\rho}\bar{l}\bar{e}(\lambda^2 + \mu^2 \sin^2 \beta)$$

$$\bar{F}_{98} = -\bar{\rho}\bar{l}\bar{e}\mu^2 \sin \beta \cos \beta$$

$$\bar{F}_{910} = (\bar{I}_\zeta + \bar{I}_\eta)\bar{l}\lambda^2 + \mu^2\bar{l} \cos 2\beta(\bar{I}_\eta - \bar{I}_\zeta) - \bar{\rho}\bar{e}\bar{e}_0\bar{l}\mu^2 \cos \beta$$

And the corresponding [E] matrix

$$[\bar{E}] = \begin{bmatrix} 1 & 0 & 0 & 0 & 0 & 0 & 0 & 0 & 0 & 0 \\ \bar{E}_{21} & 1 & 0 & 0 & 0 & 0 & 0 & 0 & 0 & 0 \\ \bar{E}_{31} & \bar{E}_{32} & \bar{E}_{33} & \bar{E}_{34} & \bar{E}_{35} & \bar{E}_{36} & \bar{E}_{37} & \bar{E}_{38} & \bar{E}_{39} & \bar{E}_{310} \\ \bar{E}_{41} & \bar{E}_{42} & \bar{E}_{43} & \bar{E}_{44} & \bar{E}_{45} & \bar{E}_{46} & \bar{E}_{47} & \bar{E}_{48} & \bar{E}_{49} & \bar{E}_{410} \\ 0 & 0 & 0 & 0 & 1 & 0 & 0 & 0 & 0 & 0 \\ 0 & 0 & 0 & 0 & \bar{E}_{65} & 1 & 0 & 0 & 0 & 0 \\ \bar{E}_{71} & \bar{E}_{72} & \bar{E}_{73} & \bar{E}_{74} & \bar{E}_{75} & \bar{E}_{76} & \bar{E}_{77} & \bar{E}_{78} & \bar{E}_{79} & \bar{E}_{710} \\ \bar{E}_{81} & \bar{E}_{82} & \bar{E}_{83} & \bar{E}_{84} & \bar{E}_{85} & \bar{E}_{86} & \bar{E}_{87} & \bar{E}_{88} & \bar{E}_{89} & \bar{E}_{810} \\ 0 & 0 & 0 & 0 & 0 & 0 & 0 & 0 & 1 & 0 \\ \bar{E}_{101} & \bar{E}_{102} & \bar{E}_{103} & \bar{E}_{104} & \bar{E}_{105} & \bar{E}_{106} & \bar{E}_{107} & \bar{E}_{108} & \bar{E}_{109} & 1 \end{bmatrix} \quad (2.20)$$

where

$$\bar{E}_{21} = \bar{t}$$

$$\bar{E}_{31} = -\frac{1}{\bar{f}_2 \bar{E} \bar{I}_1} \left\{ (\bar{a}_2 \bar{a}_6 \bar{P}_4 - \bar{a}_3 \bar{a}_8 \bar{P}_3) \cosh \bar{p} \bar{t} + [-\bar{a}_2 \bar{a}_6 \bar{P}_4 + \bar{a}_3 \bar{a}_8 (\bar{P}_3 + 1)] \cosh \bar{p}_2 \bar{t} - \bar{a}_3 \bar{a}_8 \right\}$$

$$\bar{E}_{32} = \frac{\bar{P}_3}{\bar{E} \bar{I}_1 \bar{p}_1} \sinh \bar{p}_1 \bar{t} - \frac{\bar{P}_2}{\bar{E} \bar{I}_1 \bar{p}_2} \sinh \bar{p}_2 \bar{t}$$

$$\bar{E}_{33} = -\bar{P}_3 \cosh \bar{p}_1 \bar{t} + \bar{P}_2 \cosh \bar{p}_2 \bar{t}$$

$$\bar{E}_{34} = \bar{a}_1 \bar{E} \bar{I}_1 \bar{E}_{32}$$

(2.21)

$$\bar{E}_{35} = -\frac{\gamma^2 \bar{a}_2 \bar{P}_4}{\bar{a}_3 \bar{a}_4 \bar{E} \bar{I}_2} \left(\frac{1}{\bar{p}_1} \sinh \bar{p}_1 \bar{t} - \frac{1}{\bar{p}_2} \sinh \bar{p}_2 \bar{t} \right)$$

$$\bar{E}_{36} = -\frac{\gamma^2 \bar{a}_2 \bar{P}_4}{\bar{a}_3 \bar{a}_4 \bar{E} \bar{I}_2} (\cosh \bar{p}_1 \bar{t} - \cosh \bar{p}_2 \bar{t})$$

$$\bar{E}_{37} = -\frac{\bar{a}_3 \bar{E} \bar{I}_2}{\gamma^2} \bar{E}_{35}$$

$$\bar{E}_{38} = +\frac{\bar{a}_3 \bar{E} \bar{I}_2}{\gamma^2} \bar{E}_{36}$$

$$\bar{E}_{39} = \frac{\bar{a}_2}{\bar{f}_2 (\bar{p}_1^2 - \bar{p}_2^2)} \left[(\bar{p}_1^2 - \bar{a}_3) \bar{p}_2^2 \cosh \bar{p}_1 \bar{t} - (\bar{p}_2^2 - \bar{a}_3) \bar{p}_1^2 \cosh \bar{p}_2 \bar{t} \right] - \frac{\bar{a}_2 \bar{a}_3}{\bar{f}_2}$$

$$\bar{E}_{310} = \bar{a}_2 \bar{E} \bar{I}_1 \bar{E}_{32} + \mu^2 \bar{W}^{(N)} \bar{E}_{36}$$

$$\begin{aligned} \bar{E}_{41} = & \frac{1}{\bar{f}_2 \bar{E} \bar{I}_1} \left\{ (-\bar{a}_3 \bar{a}_8 \bar{P}_3 + \bar{a}_2 \bar{a}_6 \bar{P}_4) \frac{1}{\bar{p}_1} \sinh \bar{p}_1 \bar{l} \right. \\ & \left. + \left[\bar{a}_3 \bar{a}_8 (\bar{P}_3 + 1) - \bar{a}_2 \bar{a}_6 \bar{P}_4 \right] \frac{1}{\bar{p}_2} \sinh \bar{p}_2 \bar{l} - \bar{a}_3 \bar{a}_8 \bar{l} \right\} \end{aligned}$$

$$\bar{E}_{42} = \frac{1}{\bar{E} \bar{I}_1} \left[\frac{-\bar{p}_1^2 (\bar{p}_2^2 - \bar{a}_3) + \bar{a}_3 (\bar{p}_2^2 - \bar{a}_1)}{(\bar{a}_1 - \bar{a}_3) \bar{p}_1 \bar{p}_2^2} - \frac{\bar{P}_3}{\bar{p}_1} \cosh \bar{p}_1 \bar{l} + \frac{\bar{P}_2}{\bar{p}_2} \cosh \bar{p}_2 \bar{l} \right]$$

$$\bar{E}_{43} = \bar{E} \bar{I}_1 \bar{E}_{32}$$

$$\bar{E}_{44} = - \frac{\bar{a}_3 (\bar{p}_1^2 - \bar{p}_2^2) \bar{P}_1}{\bar{p}_1 \bar{p}_2^2} - \frac{\bar{a}_1 \bar{P}_3}{\bar{p}_1^2} \cosh \bar{p}_1 \bar{l} + \frac{\bar{a}_1 \bar{P}_2}{\bar{p}_2^2} \cosh \bar{p}_2 \bar{l}$$

$$\bar{E}_{45} = \frac{\bar{a}_2 \bar{P}_4 \gamma^2}{\bar{a}_3 \bar{a}_4 \bar{p}_1 \bar{p}_2^2 \bar{E} \bar{I}_2} \left[(\bar{p}_1^2 - \bar{p}_2^2) + \bar{p}_2^2 \cosh \bar{p}_1 \bar{l} - \bar{p}_1^2 \cosh \bar{p}_2 \bar{l} \right]$$

$$\bar{E}_{46} = - \bar{E}_{35}$$

$$\bar{E}_{47} = - \frac{\bar{a}_3 \bar{E} \bar{I}_2}{\gamma^2} \bar{E}_{45}$$

$$\bar{E}_{48} = \bar{E}_{37} \quad (2.21)$$

$$\bar{E}_{49} = \frac{\bar{a}_2}{\bar{f}_2 (\bar{p}_1 - \bar{p}_2)} \left[-(\bar{p}_1^2 - \bar{a}_3) \frac{\bar{p}_2^2}{\bar{p}_1} \sinh \bar{p}_1 \bar{l} + (\bar{p}_2^2 - \bar{a}_3) \frac{\bar{p}_1^2}{\bar{p}_2} \sinh \bar{p}_2 \bar{l} \right] + \frac{\bar{a}_2 \bar{a}_3 \bar{l}}{\bar{f}_2}$$

$$\bar{E}_{410} = \bar{a}_2 \bar{E} \bar{I}_1 \bar{E}_{42} + \mu^2 \bar{W}^{(N)} \bar{E}_{46}$$

$$\bar{E}_{65} = \bar{l}$$

$$\bar{E}_{71} = \frac{\bar{a}_4}{\bar{a}_2 \bar{f}_2 \bar{E} \bar{I}_1} \left[(-\bar{a}_2 \bar{a}_6 \bar{P}_2 + \bar{a}_3 \bar{a}_8 \bar{P}_1) \bar{p}_1 \sinh \bar{p}_1 \bar{l} + (\bar{a}_2 \bar{a}_6 \bar{P}_3 - \bar{a}_3 \bar{a}_8 \bar{P}_1) \bar{p}_2 \sinh \bar{p}_2 \bar{l} \right]$$

$$\bar{E}_{72} = \frac{\bar{a}_4 \bar{P}_1}{\bar{a}_3 \bar{E} \bar{I}_1} (\cosh \bar{p}_1 \bar{l} - \cosh \bar{p}_2 \bar{l})$$

$$\bar{E}_{73} = \frac{\bar{a}_4 \bar{P}_1}{\bar{a}_2} (-\bar{p}_1 \sinh \bar{p}_1 \bar{l} + \bar{p}_2 \sinh \bar{p}_2 \bar{l})$$

$$\bar{E}_{74} = \bar{a}_1 \bar{E} \bar{I}_1 \bar{E}_{72}$$

$$\begin{aligned}
\bar{E}_{75} &= \frac{\gamma^2}{\bar{a}_3 \bar{E} \bar{I}_2} (1 - \bar{E}_{77}) \\
\bar{E}_{76} &= \frac{\gamma^2}{\bar{a}_3 \bar{E} \bar{I}_2} (-\bar{P}_2 \bar{P}_1 \sinh \bar{p}_1 \bar{l} + \bar{P}_3 \bar{P}_2 \sinh \bar{p}_2 \bar{l}) \\
\bar{E}_{77} &= \bar{P}_2 \cosh \bar{p}_1 \bar{l} - \bar{P}_3 \cosh \bar{p}_2 \bar{l} \\
\bar{E}_{78} &= \frac{\bar{a}_3 \bar{E} \bar{I}_2}{\gamma^2} \bar{E}_{76} \\
\bar{E}_{79} &= \frac{\bar{a}_4 \bar{p}_1 \bar{p}_2}{\bar{f}_2 (\bar{p}_1^2 - \bar{p}_2^2)} \left[(\bar{p}_1^2 - \bar{a}_1) \bar{p}_2^2 \sinh \bar{p}_1 \bar{l} - (\bar{p}_2^2 - \bar{a}_1) \bar{p}_1^2 \sinh \bar{p}_2 \bar{l} \right] \\
\bar{E}_{710} &= \bar{a}_2 \bar{E} \bar{I}_1 \bar{E}_{72} + \mu^2 \bar{W}^{(N)} \bar{E}_{76} \\
\bar{E}_{81} &= \frac{\bar{a}_4}{\bar{a}_2 \bar{f}_2 \bar{E} \bar{I}_1} \left[(\bar{a}_2 \bar{a}_6 \bar{P}_2 - \bar{a}_3 \bar{a}_8 \bar{P}_1) \cosh \bar{p}_1 \bar{l} + (-\bar{a}_2 \bar{a}_6 \bar{P}_3 + \bar{a}_3 \bar{a}_8 \bar{P}_1) \cosh \bar{p}_2 \bar{l} - \bar{a}_2 \bar{a}_6 \right] \\
\bar{E}_{82} &= - \frac{\bar{a}_4 \bar{P}_1}{\bar{a}_2 \bar{E} \bar{I}_1} \left(\frac{1}{\bar{p}_1} \sinh \bar{p}_1 \bar{l} + \frac{1}{\bar{p}_2} \sinh \bar{p}_2 \bar{l} \right) \\
\bar{E}_{83} &= \bar{E} \bar{I}_1 \bar{E}_{72} \\
\bar{E}_{84} &= \bar{a}_1 \bar{E} \bar{I}_1 \bar{E}_{82} \\
\bar{E}_{85} &= - \frac{\gamma^2}{\bar{a}_3 \bar{E} \bar{I}_2} (\bar{E}_{87} + \bar{l}) \\
\bar{E}_{86} &= \frac{\gamma^2}{\bar{a}_3 \bar{E} \bar{I}_2} (\bar{E}_{88} - 1) \\
\bar{E}_{87} &= - \frac{\bar{P}_2}{\bar{p}_1} \sinh \bar{p}_1 \bar{l} + \frac{\bar{P}_3}{\bar{p}_2} \sinh \bar{p}_2 \bar{l} \\
\bar{E}_{88} &= \bar{P}_2 \cosh \bar{p}_1 \bar{l} - \bar{P}_3 \cosh \bar{p}_2 \bar{l} \\
\bar{E}_{89} &= \frac{\bar{a}_4}{\bar{f}_2 (\bar{p}_1^2 - \bar{p}_2^2)} \left[-(\bar{p}_1^2 - \bar{a}_1) \bar{p}_2^2 \cosh \bar{p}_1 \bar{l} + (\bar{p}_2^2 - \bar{a}_1) \bar{p}_1^2 \cosh \bar{p}_2 \bar{l} \right] + \frac{\bar{a}_1 \bar{a}_4}{\bar{f}_2} \\
\bar{E}_{810} &= \bar{a}_2 \bar{E} \bar{I}_1 \bar{E}_{82} + \mu^2 \bar{W}^{(N)} \bar{E}_{86}
\end{aligned} \tag{2.21}$$

$$\begin{aligned}
\bar{E}_{101} &= \frac{1}{\bar{a}_2 \bar{f}_2 \bar{E} \bar{I}_1} \left[\frac{(\bar{p}_1^2 - \bar{a}_3)}{\bar{p}_1} (\bar{a}_2 \bar{a}_6 \bar{p}_2 - \bar{a}_3 \bar{a}_8 \bar{p}_1) \sinh \bar{p}_1 \bar{l} \right. \\
&\quad \left. - \frac{(\bar{p}_2^2 - \bar{a}_3)}{\bar{p}_2} (\bar{a}_2 \bar{a}_6 \bar{p}_3 - \bar{a}_3 \bar{a}_8 \bar{p}_1) \sinh \bar{p}_2 \bar{l} \right] \\
\bar{E}_{102} &= \frac{\bar{p}_1}{\bar{a}_2 \bar{p}_1^2 \bar{p}_2^2 \bar{E} \bar{I}_1} \left[\bar{a}_3 (\bar{p}_1^2 - \bar{p}_2^2) - (\bar{p}_1^2 - \bar{a}_3) \bar{p}_2^2 \cosh \bar{p}_1 \bar{l} + (\bar{p}_2^2 - \bar{a}_3) \bar{p}_1^2 \cosh \bar{p}_2 \bar{l} + \bar{a}_2 \bar{a}_3 \bar{a}_8 \bar{l} \right] \\
\bar{E}_{103} &= \frac{\bar{p}_1}{\bar{a}_2} \left[\frac{(\bar{p}_1^2 - \bar{a}_3)}{\bar{p}_1} \sinh \bar{p}_1 \bar{l} - \frac{(\bar{p}_2^2 - \bar{a}_3)}{\bar{p}_2} \sinh \bar{p}_1 \bar{l} \right] \\
\bar{E}_{104} &= \bar{a}_1 \bar{E} \bar{I}_1 \bar{E}_{102} \\
\bar{E}_{105} &= \frac{\gamma^2 \bar{p}_4}{\bar{a}_3 \bar{a}_4 \bar{p}_1^2 \bar{p}_2^2 \bar{E} \bar{I}_2} \left[-\bar{a}_1 (\bar{p}_1^2 - \bar{p}_2^2) + (\bar{p}_1^2 - \bar{a}_1) \bar{p}_2^2 \cosh \bar{p}_1 \bar{l} - (\bar{p}_2^2 - \bar{a}_1) \bar{p}_1^2 \cosh \bar{p}_2 \bar{l} \right] \quad (2.21) \\
\bar{E}_{106} &= \frac{\gamma^2 \bar{p}_4}{\bar{a}_3 \bar{a}_4 \bar{E} \bar{I}_2} \left[\frac{(\bar{p}_1^2 - \bar{a}_1)}{\bar{p}_1} \sinh \bar{p}_1 \bar{l} - \frac{\bar{p}_2^2 - \bar{a}_1}{\bar{p}_2} \sinh \bar{p}_2 \bar{l} \right] \\
\bar{E}_{107} &= - \frac{\bar{a}_3 \bar{E} \bar{I}_2 \bar{E}_{105}}{\gamma^2} \\
\bar{E}_{108} &= \frac{\bar{a}_3 \bar{E} \bar{I}_2 \bar{E}_{106}}{\gamma^2} \\
\bar{E}_{109} &= \frac{1}{\bar{f}_2} \left\{ -\bar{a}_1 \bar{a}_3 \bar{l} - \frac{1}{(\bar{p}_1^2 - \bar{p}_2^2)} \left[(\bar{p}_1^2 - \bar{a}_1)(\bar{p}_1^2 - \bar{a}_3) \frac{\bar{p}_2^2}{\bar{p}_1} \sinh \bar{p}_1 \bar{l} \right. \right. \\
&\quad \left. \left. + (\bar{p}_2^2 - \bar{a}_1)(\bar{p}_2^2 - \bar{a}_3) \frac{\bar{p}_1^2}{\bar{p}_2} \sinh \bar{p}_2 \bar{l} \right] \right\} \\
\bar{E}_{1010} &= \frac{1}{\bar{p}_1^2 \bar{p}_2^2} \left\{ \frac{\bar{a}_1}{(\bar{a}_1 - \bar{a}_3)} \left[\bar{p}_1^2 (\bar{p}_2^2 - \bar{a}_3) - \bar{a}_3 (\bar{p}_2^2 - \bar{a}_1) \right] + \bar{p}_1 \left[-(\bar{p}_1^2 - \bar{a}_3) \bar{p}_2^2 \cosh \bar{p}_1 \bar{l} \right. \right. \\
&\quad \left. \left. + (\bar{p}_2^2 - \bar{a}_3) \bar{p}_1^2 \cosh \bar{p}_2 \bar{l} \right] \right\} + \mu^2 \bar{W}^{(N)} \bar{E}_{106}
\end{aligned}$$

The nondimension quantities used above are defined as follows:

$$\begin{aligned}
\bar{a}_1 &= \mu^2 \frac{\bar{T}}{\bar{E} \bar{I}_1} \\
\bar{a}_2 &= \mu^2 \frac{\bar{U}^{(N)}}{\bar{E} \bar{I}_1}
\end{aligned} \quad (2.22)$$

$$\bar{a}_3 = \mu^2 \gamma^2 \frac{\bar{T}}{\bar{E}\bar{I}_2}$$

$$\bar{a}_4 = -\gamma \sqrt{\bar{Y}} \sqrt{1/\bar{E}\bar{I}_2}$$

$$\bar{a}_6 = \mu^2 \bar{U}^{(N)}$$

$$\bar{a}_7 = -\frac{1}{\gamma} \sqrt{\bar{Y}} \sqrt{\bar{E}\bar{I}_2}$$

$$\bar{a}_8 = \bar{A}^{(N)}$$

$$\bar{f}_0 = \bar{A} - \bar{Y} = \bar{a}_8 - \bar{a}_4 \bar{a}_7$$

$$\bar{f}_1 = \mu^2 \left[\frac{\mu^2 \bar{U}^2}{\bar{E}\bar{I}_1} - \bar{A}\bar{T} \left(\frac{1}{\bar{E}\bar{I}_1} + \frac{\gamma^2}{\bar{E}\bar{I}_2} \right) + \frac{\bar{T}\bar{Y}}{\bar{E}\bar{I}_1} \right] = \bar{a}_2 \bar{a}_6 - \bar{a}_8 (\bar{a}_1 + \bar{a}_3) + \bar{a}_1 \bar{a}_4 \bar{a}_7$$

$$\bar{f}_2 = \mu^4 \gamma^2 \frac{\bar{T}}{\bar{E}\bar{I}_1 \bar{E}\bar{I}_2} (\bar{T}\bar{A} - \mu^2 \bar{U}^2) = \bar{a}_3 (\bar{a}_1 \bar{a}_8 - \bar{a}_2 \bar{a}_6) \quad (2.22)$$

$$\bar{p}_1^2 = -\frac{\bar{f}_1}{2\bar{f}_0} + \sqrt{\left(\frac{\bar{f}_1}{2\bar{f}_0}\right)^2 - \frac{\bar{f}_2}{\bar{f}_0}}$$

$$\bar{p}_2^2 = -\frac{\bar{f}_1}{2\bar{f}_0} - \sqrt{\left(\frac{\bar{f}_1}{2\bar{f}_0}\right)^2 - \frac{\bar{f}_2}{\bar{f}_0}}$$

$$\bar{P}_1 = \frac{(\bar{p}_1^2 - \bar{a}_1)(\bar{p}_2^2 - \bar{a}_1)}{(\bar{a}_1 - \bar{a}_3)(\bar{p}_1^2 - \bar{p}_2^2)}$$

$$\bar{P}_2 = \frac{(\bar{p}_1^2 - \bar{a}_1)(\bar{p}_2^2 - \bar{a}_3)}{(\bar{a}_1 - \bar{a}_3)(\bar{p}_1^2 - \bar{p}_2^2)}$$

$$\bar{P}_3 = \frac{(\bar{p}_1^2 - \bar{a}_3)(\bar{p}_2^2 - \bar{a}_1)}{(\bar{a}_1 - \bar{a}_3)(\bar{p}_1^2 - \bar{p}_2^2)}$$

$$\bar{P}_4 = \frac{(\bar{p}_1^2 - \bar{a}_3)(\bar{p}_2^2 - \bar{a}_3)}{(\bar{a}_1 - \bar{a}_3)(\bar{p}_1^2 - \bar{p}_2^2)}$$

$$\bar{U}^{(N)} = \sin \beta_N \sum_{i=1}^N \bar{l}_i \bar{\rho}_i \bar{e}_i \bar{x}_i \sin \beta_i + \cos \beta_N \sum_{i=1}^N \bar{l}_i \bar{\rho}_i \bar{e}_i \bar{x}_i \cos \beta_i$$

$$\bar{W}^{(N)} = -\cos \beta_N \sum_{i=1}^N \bar{l}_i \bar{\rho}_i \bar{e}_i \bar{x}_i \sin \beta_i + \sin \beta_N \sum_{i=1}^N \bar{l}_i \bar{\rho}_i \bar{e}_i \bar{x}_i \cos \beta_i \quad .$$

where N denotes the number of masses outboard of the bay under consideration.

The $\{\bar{d}\}$ matrix has the components

$$\begin{aligned}
 \bar{d}_1 &= -\bar{l}\bar{\rho}\mu^2 \sin \beta(\bar{e}_0 + \bar{e} \cos \beta) \\
 \bar{d}_2 &= \bar{d}_3 = \bar{d}_4 = \bar{d}_7 = \bar{d}_8 = \bar{d}_{10} = 0 \\
 \bar{d}_5 &= \bar{l}\bar{\rho}\mu^2 \cos \beta(\bar{e}_0 + \bar{e} \cos \beta) \\
 \bar{d}_6 &= -\bar{l}\bar{\rho}\bar{x}\bar{e}\mu^2 \\
 \bar{d}_9 &= (\bar{l}_\eta - \bar{l}_\zeta)\bar{l}\mu^2 \sin \beta \cos \beta - \bar{l}\bar{\rho}\bar{e}\bar{e}_0\mu^2 \sin \beta,
 \end{aligned} \tag{2.23}$$

and the components of $\{g\}$ are

$$g_i = \mu^2(\bar{E}_{i2}\bar{l}\bar{e}_A + \bar{E}_{i9}\bar{l}k_A\bar{\beta}^2) \tag{2.24}$$

For the case of zero rotational velocity, the $[\bar{F}]$ matrix is obtained directly by substitution of $\mu = 0$. When this substitution is made in the $[\bar{E}]$ matrix, some of the elements are found to be of indeterminate form and a limiting process must be applied. This results in:

$$\begin{aligned}
 \bar{E}_{21} &= \bar{l} \\
 \bar{E}_{31} &= -\frac{\bar{l}^2}{2\bar{E}\bar{l}_1} \\
 \bar{E}_{32} &= -\frac{\bar{l}}{\bar{E}\bar{l}_1} \\
 \bar{E}_{33} &= 1 \\
 \bar{E}_{34} &= 0 \\
 \bar{E}_{41} &= \frac{\bar{l}^3}{6\bar{E}\bar{l}_1}
 \end{aligned} \tag{2.25}$$

$$\bar{E}_{42} = -\bar{E}_{31}$$

$$\bar{E}_{43} = -\bar{l}$$

$$\bar{E}_{44} = 1$$

$$\bar{E}_{65} = \bar{l}$$

$$\bar{E}_{75} = -\frac{\gamma^2 \bar{l}^2}{2\bar{E}I_2} \left(\frac{\bar{A}}{\bar{A}-\bar{Y}} \right)$$

$$\bar{E}_{76} = -\frac{\gamma^2 \bar{l}}{\bar{E}I_2} \left(\frac{\bar{A}}{\bar{A}-\bar{Y}} \right)$$

$$\bar{E}_{77} = 1$$

$$\bar{E}_{78} = 0$$

$$\bar{E}_{79} = -\frac{\bar{C}\gamma^2 \bar{l}}{\bar{E}I_2} \left(\frac{\bar{A}}{\bar{A}-\bar{Y}} \right)$$

$$\bar{E}_{85} = \frac{\gamma^2 \bar{l}^3}{6\bar{E}I_2} \left(\frac{\bar{A}}{\bar{A}-\bar{Y}} \right)$$

(2.25)

$$\bar{E}_{86} = -\bar{E}_{75}$$

$$\bar{E}_{87} = -\bar{l}$$

$$\bar{E}_{88} = 1$$

$$\bar{E}_{89} = \frac{\bar{C}\gamma^2 \bar{l}^2}{2\bar{E}I_2} \left(\frac{\bar{A}}{\bar{A}-\bar{Y}} \right)$$

$$\bar{E}_{105} = -\bar{E}_{89}$$

$$\bar{E}_{106} = \bar{E}_{79}$$

$$\bar{E}_{107} = 0$$

$$\bar{E}_{108} = 0 \quad (2.25)$$

$$\bar{E}_{109} = -\frac{\bar{I}}{A+Y}$$

NUMERICAL RESULTS

A program of computations was performed for two representative cantilever blades. The properties of these blades are given in Table 1. They were chosen to have the same bending properties as blades for which numerical results are reported in Ref. 1. For these two, the section constants I_1 , I_2 , B_1 , B_2 , GJ_e , k_A correspond to those for a thin-walled rectangular section, and it was assumed that some nonstructural mass was distributed in such a way as to provide an offset between the mass and elastic axes, and to provide sufficient mass moment of inertia to make the uncoupled first torsional frequency and the second uncoupled flapwise frequency coincide. The result in both cases is a lightly coupled system as far as flapwise bending-torsion is concerned.

In both cases the blades were divided into ten segments, the cantilever root condition was applied, and the four lowest frequencies were determined. A range of values of pretwist and rotational velocity was chosen, and the results are presented in Figs. 2.4-2.6. In addition, results for beam No. 2 with rotary inertia neglected are presented in Fig. 2.6, and with centrifugal force coupling neglected in Fig. 2.7.

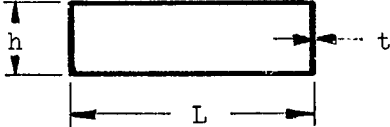
DISCUSSION OF RESULTS

The influence of twist on the natural frequencies of nonrotating blades is shown in Fig. 2.4. The fundamental frequency in each case is almost completely unaffected. The higher frequencies are affected by the coupling between flapwise bending and torsion, and between all three types of deformation when twist is introduced.

The combined effects of rotation and twist on blade No. 1 are illustrated in Fig. 2.5. In the untwisted, nonrotating case the fundamental mode is identified as predominantly flapwise bending; the second mode is uncoupled chordwise bending; and the third and fourth modes are coupled flapwise bending and torsion. The effect of rotation and twist is to couple the first two modes. A comparison of the results in Fig. 2.5 with results in Ref. 1 for a beam with the same bending properties but with torsion neglected shows that essentially no change has been introduced by the presence of torsion. The fourth frequency in Fig. 2.5 differs slightly from the third frequency for the beam in Ref. 1,

TABLE I

BEAM PROPERTIES

Beam No.	1	2
		
h/L	$2.285 \cdot 10^{-1}$	$6.225 \cdot 10^{-2}$
h/R	$1.000 \cdot 10^{-2}$	$1.000 \cdot 10^{-2}$
\bar{e}	$0.25 L$	$0.15 L$
\bar{e}_O	0	0
\bar{k}_A	0.015522	0.04926
β_T	0	0
γ^2	$1.000 \cdot 10^{-1}$	$1.000 \cdot 10^{-2}$
$I_1[\text{in.}^4]$	$2.355 h^3 t$	$8.1987 h^3 t$
$I_2[\text{in.}^4]$	$(2.355 \cdot 10) h^3 t$	$(8.1987 \cdot 10^2) h^3 t$
$B_1[\text{in.}^6]$	$32.692 h^5 t$	$15.345 h^5 t$
$B_2[\text{in.}^5]$	0	0
\overline{GJ}_e^*	1.153	1.405
\bar{I}_η	$2.190 \cdot 10^{-5}$	$2.402 \cdot 10^{-5}$
\bar{I}_ζ	$5.832 \cdot 10^{-3}$	$7.114 \cdot 10^{-3}$

*Aluminum is assumed.

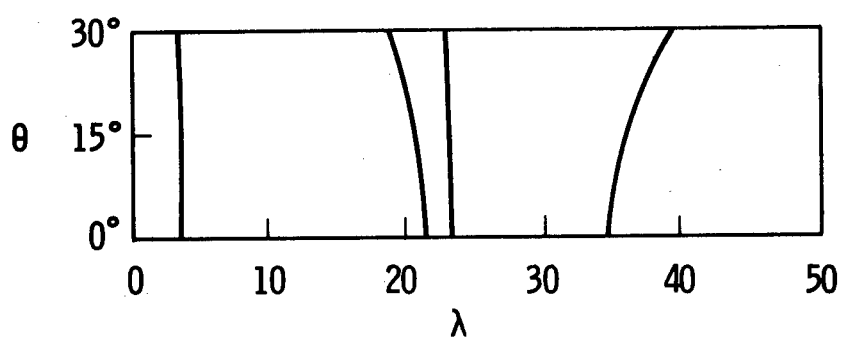
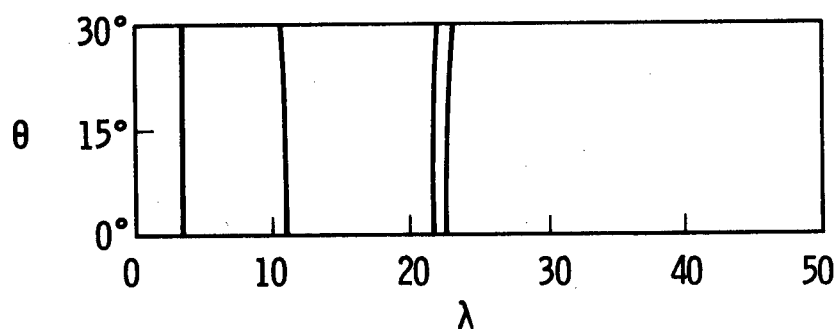


Fig. 2.4. Effect of twist on natural frequencies of nonrotating blades.

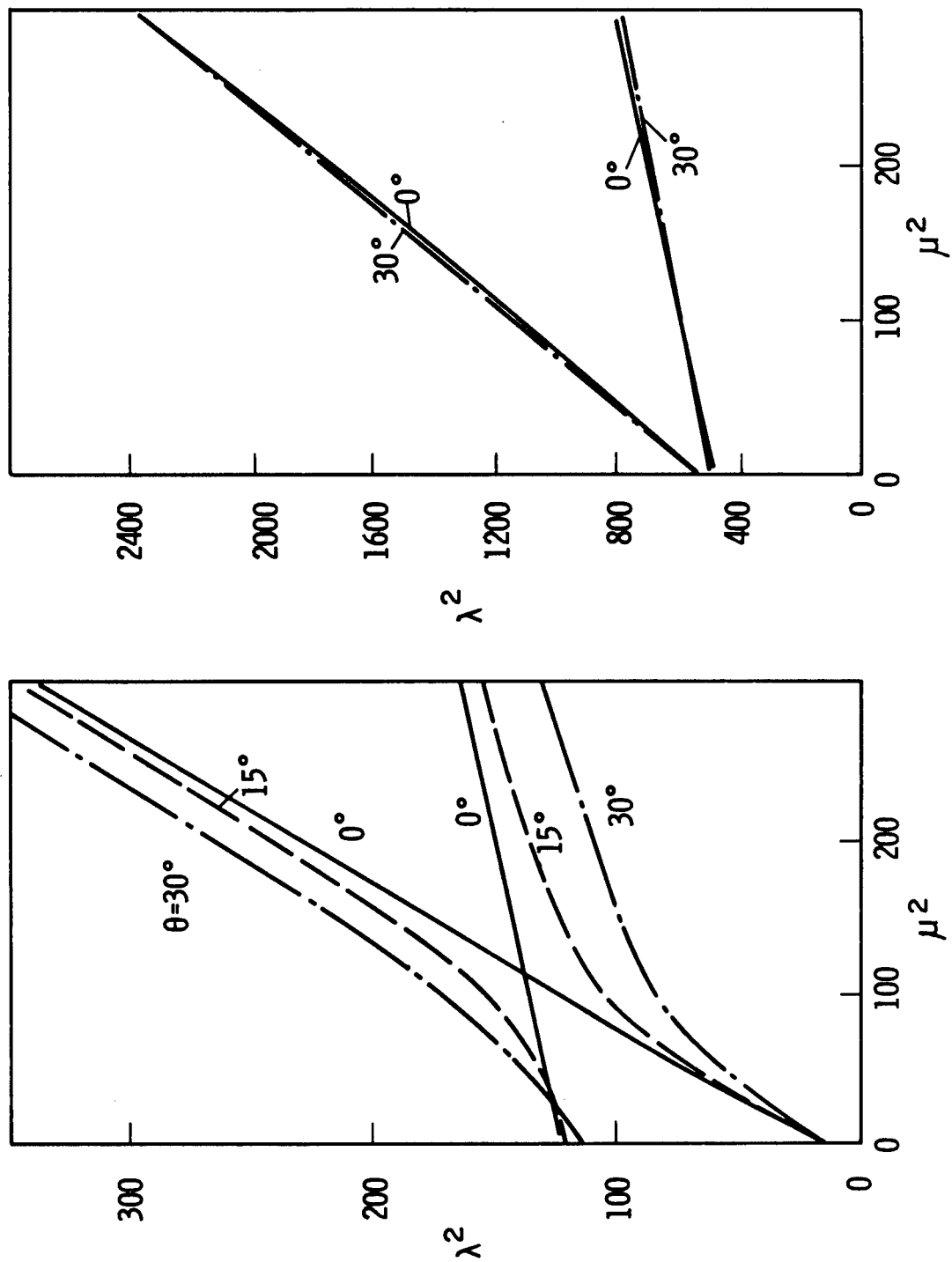


Fig. 2.5. Natural frequencies of rotating blade No. 1.

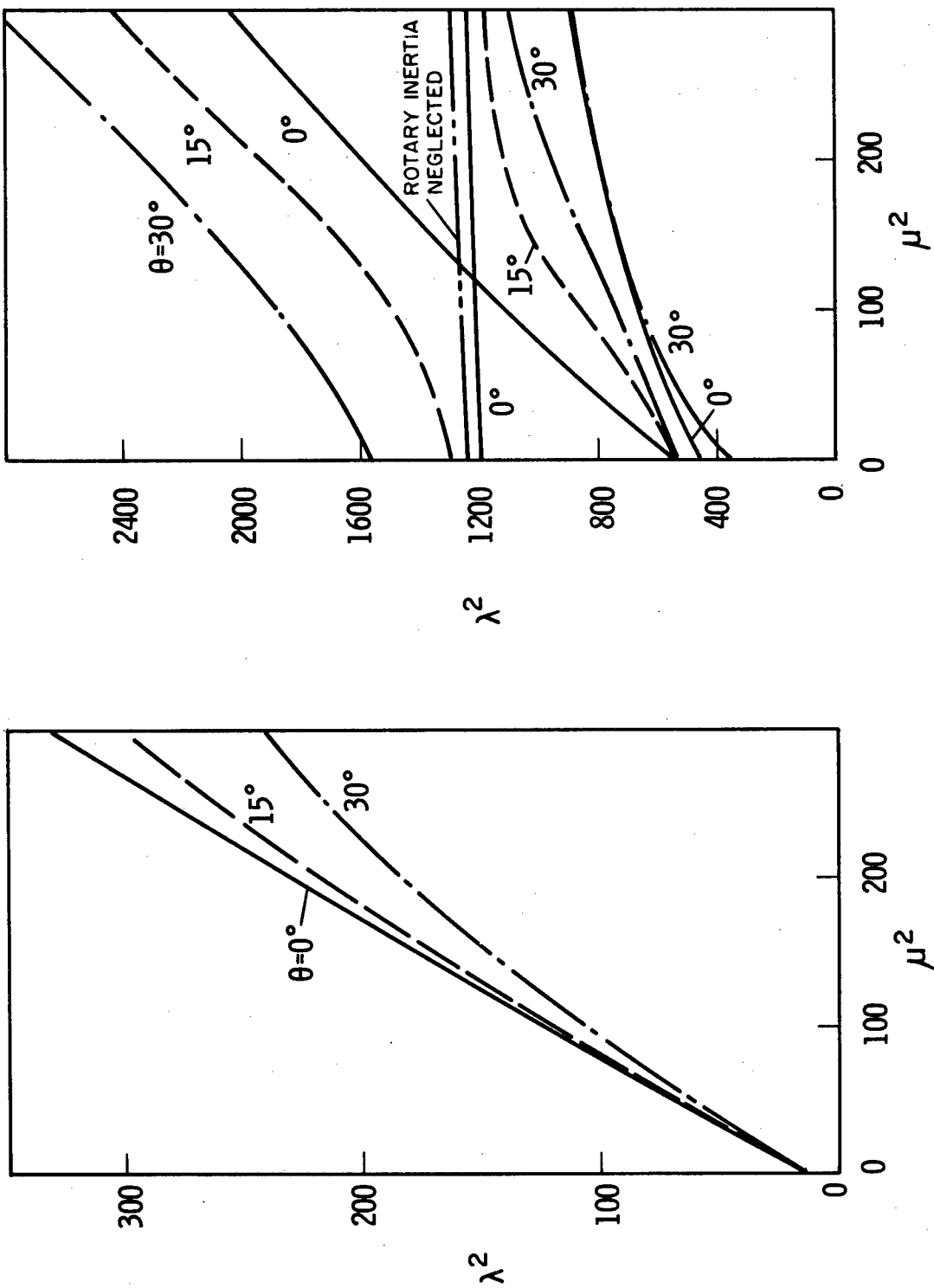


Fig. 2.6. Natural frequencies of rotating blade No. 2.

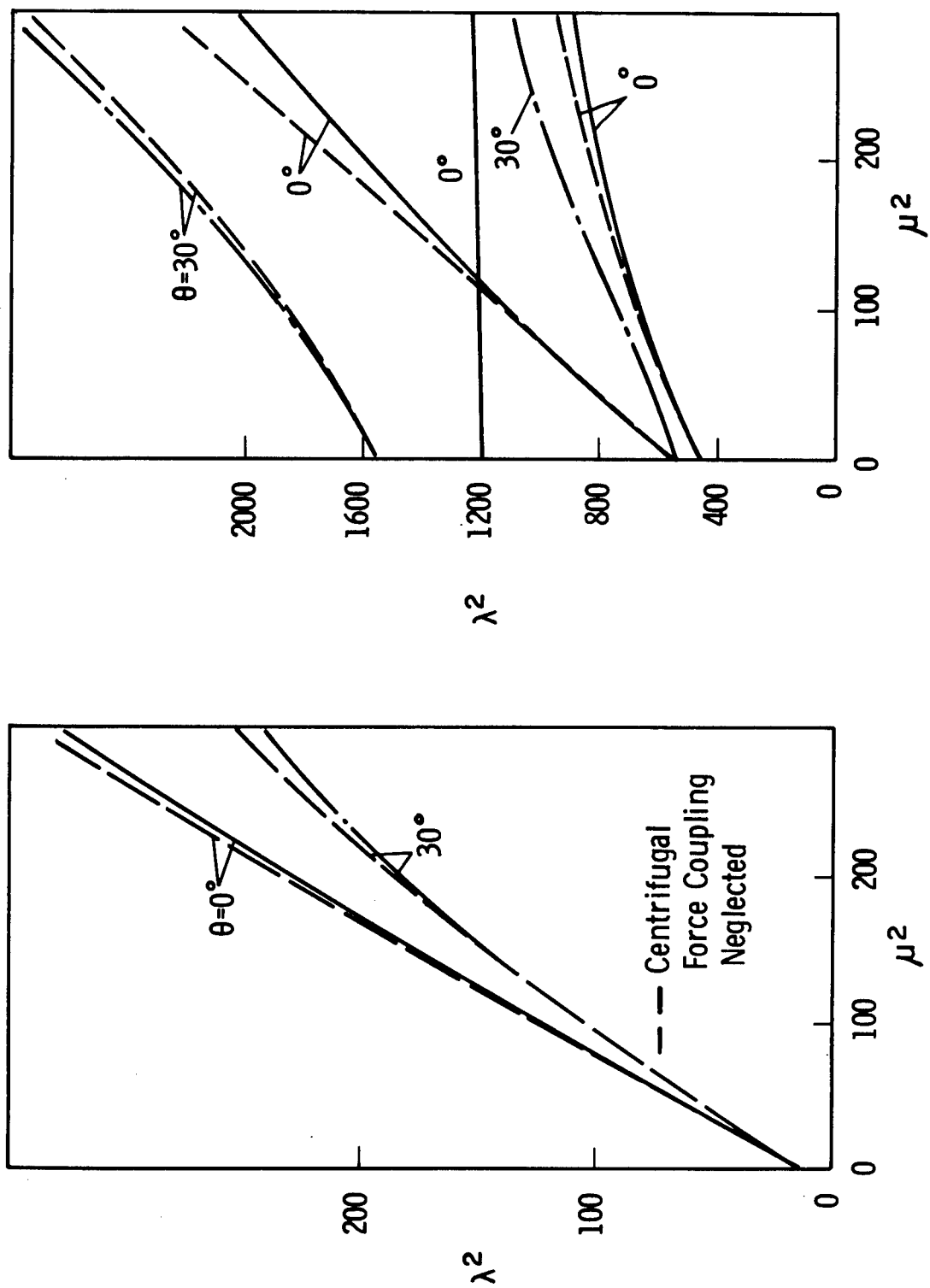


Fig. 2.7. Effects of centrifugal force coupling on blade No. 2.

while the third frequency in Fig. 2.5 is a new one introduced by the presence of torsion. It is seen that twist has little effect on the third and fourth frequencies shown in Fig. 2.5. A small difference between the results in Ref. 1 and the present results is introduced by the inclusion of rotary inertia in the present analysis.

The results for blade No. 2 presented in Fig. 2.6 show that the fundamental frequency is essentially unchanged by the presence of torsion when compared with results for a similar blade reported in Ref. 1. For this blade the fundamental mode is predominantly flapwise bending. The second and third modes for the untwisted, nonrotating blade are coupled flapwise bending and torsion, and the fourth mode is uncoupled chordwise bending. When rotation and twist are added, the three higher modes exhibit considerable coupling, and it becomes difficult to reach any general conclusions. When compared with the results in Ref. 1 for a similar blade without torsion, it is seen that the effect of the presence of torsion is to introduce a new frequency and to modify the other two frequencies a moderate amount. That these two frequencies are not modified more by the presence of torsion is to be expected since the coupling for this blade (and also for blade No. 1), as represented by the amount of offset between the mass and elastic axes, is relatively small.

The neglect of rotary inertia has a negligible effect on the natural frequencies except for those cases in which there is chordwise bending. For example, in the case of the untwisted beam No. 2 the only frequency which is appreciably affected is the uncoupled chordwise bending frequency. The magnitude of this effect is shown in Fig. 2.6.

The effects of centrifugal force coupling on beam No. 2 are shown in Fig. 2.7. Curves with and without centrifugal force coupling are shown for $\theta = 0^\circ$ and 30° . Only the $\theta = 0^\circ$ case is shown for the second frequency to avoid confusion in plotting. The $\theta = 30^\circ$ case for the second frequency is modified by a slightly smaller amount. The $\theta = 0^\circ$ case which represents uncoupled chordwise bending (the fourth frequency for the nonrotating beam) is essentially unaffected, as is the $\theta = 30^\circ$ case for the third coupled frequency. It can be seen from these results that centrifugal force coupling can have an appreciable effect on some of the vibration characteristics.

3. SIMPLE MODEL ANALYSIS

SYMBOLS

a_1, a_2	functions defined immediately following Eq. (3.13)
e	offset of mass c.g. from supporting rod, positive forward
\bar{e}	nondimensional form of e , \bar{e}/r
$\vec{i}, \vec{j}, \vec{k}$	unit vectors along the x, y, z axes respectively
I	moment of inertia of mass m about supporting rod
I_O	moment of inertia of mass m about its own c.g.
I_F	moment of inertia of flywheel
K	kinetic energy of system
k_θ	stiffness of bending spring
k_ϕ	stiffness of torsion spring
m	mass
M_T	shaft torque
\bar{M}_T	nondimensional form of M_T , $M_T/mr^2\Omega^2$
p	differential operator
r	length of supporting rod from shaft to mass m
\vec{R}	radius vector from origin to element of mass dm
t	time
U	potential energy of system
\vec{v}	velocity vector of mass element dm
v	magnitude of \vec{v}

x, y, z	axes fixed to supporting rod and mass assembly
y	y-coordinate of mass element dm
x_F, y_F, z_F	stationary axes
α	orientation angle of bending hinge axis
β	angle simulating built-in twist
γ	built-in coning angle
ϵ	phase lag of motion in ϕ -coordinate relative to motion in θ -coordinate
θ	elastic displacement about bending hinge
θ_s	pseudo-static value of θ
$\bar{\theta}$	departure of θ from θ_s
$\bar{\theta}_0$	amplitude of $\bar{\theta}$, also initial value of $\bar{\theta}$
$\bar{\rho}$	nondimensional radius of gyration of mass m about supporting rod, $\sqrt{I/mr^2}$
$\bar{\rho}_0$	nondimensional radius of gyration of mass m about its own c.g., $\sqrt{I_0/mr^2}$
τ	nondimensional form of t , Ωt
ϕ	elastic displacement about torsion hinge
ϕ_s	pseudo-static value of ϕ
$\bar{\phi}$	departure of ϕ from ϕ_s
$\bar{\phi}_0$	initial value of $\bar{\phi}$
$\bar{\phi}'_0$	initial value of $\bar{\phi}'$
$\bar{\phi}_1$	amplitude of $\bar{\phi}$
ψ	angular displacement of shaft
$\vec{\omega}$	angular velocity vector of x, y, z frame

$\omega_x, \omega_y, \omega_z$	components of $\vec{\omega}$ along the x,y,z axes, respectively
$\bar{\omega}$	natural frequency of characteristic oscillation
$\bar{\omega}_1, \bar{\omega}_2$	first and second natural frequencies of characteristic oscillation
Ω	rotational velocity of shaft

DESCRIPTION OF THE MODEL

In order to examine some effects of nonlinearity and Coriolis forces in the free vibrations of a rotating elastic blade in coupled bending and torsion and to consider the effects of certain parameters on the static deformation of the rotating blade, a simple model with a small number of degrees of freedom is set up and analyzed.

The model consists of a rigid weightless rod on one end of which is mounted a mass and the other end of which is connected to a rotating shaft. The connection to the shaft is through a hinge with axis normal to the rod and set at an angle to the shaft. A spring, restraining motion about this hinge, simulates bending stiffness. In addition, the rod is free to rotate about its own axis against the action of a spring, which simulates torsional stiffness. The mass is assumed to be distributed along a line normal to the rod, simulating the major principal axis of a blade cross section, with its center of gravity displaced from the rod, simulating an offset of the mass axis of the blade from the elastic axis.

The orientation of the model relative to a set of fixed axes and the generalized coordinates defining its configuration are shown in Fig. 3.1. The final orientation is reached by aligning the model initially with the fixed axes and then executing a sequence of rotations. The fixed axes x_F, y_F, z_F form an orthogonal set oriented so that the x_F -axis is coincident with the shaft centerline. Their origin is at the intersection of the rod and the shaft centerline and is coincident with the origin of the model axes x, y, z . The x -axis lies along the rod, the y -axis is parallel to the line along which the mass lies, and the z -axis completes the orthogonal set.

The model is initially aligned so that the x, y, z axes are coincident with the x_F, y_F, z_F axes, respectively. The following rotations, positive in the right-handed sense, of the x, y, z frame are then executed in sequence:

1. A rotation about the z_F -axis through the angle ψ to the position x_1, y_1, z_1 . ψ then defines the shaft rotation.
2. A rotation about the y_1 -axis through the angle $-\gamma$ to the position x_2, y_2, z_2 . $-\gamma$ then defines a built-in coning angle.

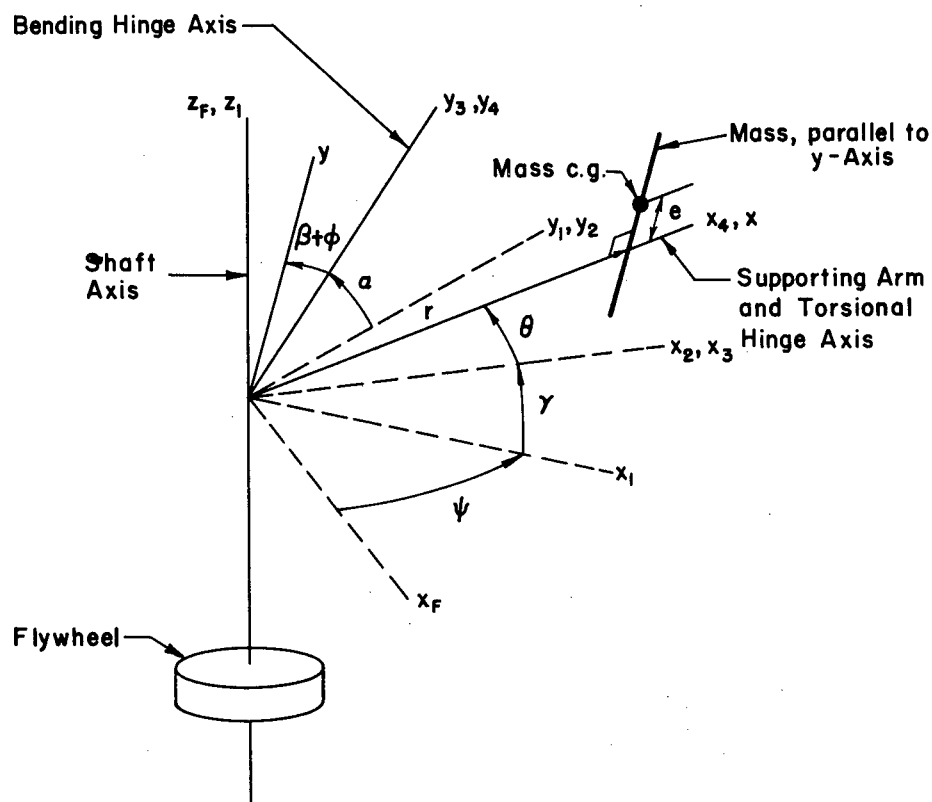


Fig. 3.1. Model coordinates.

3. A rotation about the x_2 -axis through the angle α to the position x_3, y_3, z_3 . The y_3 -axis then defines the position of the hinge axis.
4. A rotation about the y_3 -axis through the angle $-\theta$ to the position x_4, y_4, z_4 . This represents a rotation about the hinge axis simulating bending displacement.
5. A rotation about the x_4 -axis through the angles β and ϕ in sequence to the final position x, y, z . The angle β simulates built-in twist, and the angle ϕ elastic twist.

The angles α, β , and γ are constants and constitute parameters in the problem. The angles ψ, θ , and ϕ are generalized coordinates representing shaft rotation, bending, and torsional displacement, respectively.

DERIVATION OF THE EQUATIONS OF MOTION

The equations governing the motion of the model are now derived using

Lagrange's equation. Toward this end it is necessary to obtain an expression for the kinetic energy of the system in terms of the generalized coordinates.

Assuming a flywheel of moment of inertia I_F to be mounted on the shaft, and defining m as the magnitude of the mass mounted on the rod, the kinetic energy of the system may be written,

$$K = \frac{1}{2} I_F \dot{\psi}^2 + \frac{1}{2} \int_m v^2 dm \quad (3.1)$$

where v is the magnitude of the velocity vector \vec{v} of an element of the mass m .

\vec{v} may be developed from the relation,

$$\vec{v} = \vec{\omega} \times \vec{R} \quad (3.2)$$

where $\vec{\omega}$ is the angular velocity vector of the x, y, z frame and \vec{R} is the radius vector of dm . Substituting

$$\vec{\omega} = \omega_x \vec{i} + \omega_y \vec{j} + \omega_z \vec{k} \quad (3.3)$$

$$\vec{R} = r \vec{i} + y \vec{j} \quad (3.4)$$

where $\vec{i}, \vec{j}, \vec{k}$ are unit vectors along the x, y, z axes, respectively, into Eq. (3.2) the following is obtained,

$$\vec{v} = -y\omega_z \vec{i} + r\omega_z \vec{j} + (y\omega_x - r\omega_y) \vec{k} \quad (3.5)$$

Thus,

$$v^2 = y^2 \omega_z^2 + r^2 \omega_z^2 + (y\omega_x - r\omega_y)^2 \quad (3.6)$$

and Eq. (3.1) may now be written,

$$K = \frac{1}{2} I_F \dot{\psi}^2 + \frac{1}{2} m r^2 (\omega_y^2 + \omega_z^2) + \frac{1}{2} I (\omega_x^2 + \omega_z^2) - m r \omega_x \omega_y \quad (3.7)$$

where I is the moment of inertia of m about the axis of the supporting rod and e is the offset, in the positive direction of y , of the center of gravity of m from the axis of the supporting rod.

Expressions for ω_x , ω_y , and ω_z are now developed by resolving the angular velocities $\dot{\psi}$, $\dot{\theta}$ and $\dot{\phi}$ into components referred to the x , y , z axes. This is accomplished by a succession of rotations of the reference frame in the order presented earlier, expressed in the form of matrix transformations⁸ as follows,

$$\begin{aligned}
 \begin{Bmatrix} \omega_x \\ \omega_y \\ \omega_z \end{Bmatrix} &= \begin{bmatrix} 1 & 0 & 0 \\ 0 & \cos(\beta+\phi) & \sin(\beta+\phi) \\ 0 & -\sin(\beta+\phi) & \cos(\beta+\phi) \end{bmatrix} \begin{bmatrix} \cos \theta & 0 & \sin \theta \\ 0 & 1 & 0 \\ -\sin \theta & 0 & \cos \theta \end{bmatrix} \begin{bmatrix} 1 & 0 & 0 \\ 0 & \cos \alpha & \sin \alpha \\ 0 & -\sin \alpha & \cos \alpha \end{bmatrix} \begin{bmatrix} \cos \beta & 0 & \sin \beta \\ 0 & 1 & 0 \\ -\sin \beta & 0 & \cos \beta \end{bmatrix} \begin{Bmatrix} 0 \\ 0 \\ \dot{\psi} \end{Bmatrix} \\
 &+ \begin{bmatrix} 1 & 0 & 0 \\ 0 & \cos(\beta+\phi) & \sin(\beta+\phi) \\ 0 & -\sin(\beta+\phi) & \cos(\beta+\phi) \end{bmatrix} \begin{Bmatrix} 0 \\ \dot{\theta} \\ 0 \end{Bmatrix} + \begin{Bmatrix} 0 \\ 0 \\ 0 \end{Bmatrix} + \begin{Bmatrix} \dot{\phi} \\ 0 \\ 0 \end{Bmatrix} \\
 &= \begin{Bmatrix} \dot{\psi}(\cos \theta \sin \gamma + \sin \theta \cos \alpha \cos \gamma) + \dot{\phi} \\ \dot{\psi}(\cos(\beta+\phi) \sin \alpha \cos \gamma + \sin(\beta+\phi)(-\sin \theta \sin \gamma + \cos \theta \cos \alpha \cos \gamma)) - \dot{\theta} \cos(\beta+\phi) \\ \dot{\psi}(-\sin(\beta+\phi) \sin \alpha \cos \gamma + \cos(\beta+\phi)(-\sin \theta \sin \gamma + \cos \theta \cos \alpha \cos \gamma)) + \dot{\theta} \sin(\beta+\phi) \end{Bmatrix} \quad (3.8)
 \end{aligned}$$

Neglecting gravity forces, the potential energy of the system may be written as follows,

$$U = \frac{1}{2} k_{\theta} \theta^2 + \frac{1}{2} k_{\phi} \phi^2 \quad (3.9)$$

where k_{θ} and k_{ϕ} are the spring constants of the springs restraining motion in θ and ϕ coordinates.

Substitution of Eqs. (3.7), (3.8) and (3.9) into Lagrange's equation,

$$\frac{d}{dt} \left(\frac{\partial K}{\partial \dot{q}_i} \right) - \frac{\partial K}{\partial q_i} + \frac{\partial U}{\partial q_i} = 0 \quad (i=1,2,3) \quad (3.10)$$

where $q_1 = \theta$, $q_2 = \phi$, $q_3 = \psi$, yields the following differential equations,

$$\begin{aligned} & [mr^2 + I \sin^2(\beta + \phi)] \ddot{\theta} + [mre \cos(\beta + \phi)] \ddot{\phi} + \left[-mr^2 \sin \alpha \cos \gamma + mre a_2 \cos(\beta + \phi) \right. \\ & \left. + I \sin(\beta + \phi) \{-\sin(\beta + \phi) \sin \alpha \cos \gamma + a_1 \cos(\beta + \phi)\} \right] \ddot{\psi} \\ & + \left[-2I \sin(\beta + \phi) \{\cos(\beta + \phi) \sin \alpha \cos \gamma + a_1 \sin(\beta + \phi)\} - 2mre a_2 \sin(\beta + \phi) \right] \dot{\phi} \dot{\psi} \\ & + [2I \sin(\beta + \phi) \cos(\beta + \phi)] \dot{\theta} \dot{\phi} + [-rme \sin(\beta + \phi)] \dot{\phi}^2 \\ & + \left[mr^2 a_1 a_2 + mre \{a_1 \cos(\beta + \phi) \sin \alpha \cos \gamma + (a_1^2 - a_2^2) \sin(\beta + \phi)\} \right. \\ & \left. - I a_2 \sin(\beta + \phi) \{\cos(\beta + \phi) \sin \alpha \cos \gamma + a_1 \sin(\beta + \phi)\} \right] \dot{\psi}^2 \\ & + k_{\theta} \theta = 0 \end{aligned} \quad (3.11)$$

$$\begin{aligned}
& [mre \cos(\beta+\phi)]\ddot{\theta} + I\ddot{\phi} + [Ia_2 - mre(\cos(\beta+\phi)\sin\alpha \cos\gamma + a_1 \sin(\beta+\phi))] \ddot{\psi} \\
& + [2mrea_2 \sin(\beta+\phi) + 2I \sin(\beta+\phi)(\cos(\beta+\phi)\sin\alpha \cos\gamma + a_1 \sin(\beta+\phi))] \dot{\theta}\dot{\psi} \\
& + [-I \sin(\beta+\phi)\cos(\beta+\phi)]\dot{\theta}^2 \\
& + [mrea_2(-\sin(\beta+\phi)\sin\alpha \cos\gamma + a_1 \cos(\beta+\phi))] \\
& + I[-\sin(\beta+\phi)\sin\alpha \cos\gamma + a_1 \cos(\beta+\phi)]\{\cos(\beta+\phi)\sin\alpha \cos\gamma + a_1 \sin(\beta+\phi)\} \dot{\psi}^2 \\
& + k_\phi \phi = 0
\end{aligned} \tag{3.12}$$

$$\begin{aligned}
& [-mr^2 \sin\alpha \cos\gamma + mrea_2 \cos(\beta+\phi) + I \sin(\beta+\phi)(-\sin(\beta+\phi)\sin\alpha \cos\gamma + a_1 \cos(\beta+\phi))] \ddot{\theta} \\
& + [Ia_2 - mre(\cos(\beta+\phi)\sin\alpha \cos\gamma + a_1 \sin(\beta+\phi))] \ddot{\phi} \\
& + [I_F + mr^2(\sin^2\alpha \cos^2\gamma + a_1^2) - 2mrea_2(\cos(\beta+\phi)\sin\alpha \cos\gamma + a_1 \sin(\beta+\phi))] \\
& + Ia_2^2 + I(-\sin(\beta+\phi)\sin\alpha \cos\gamma + a_1 \cos(\beta+\phi))^2 \ddot{\psi} \\
& + [-2mr^2 a_1 a_2 + 2mre(a_2^2 \sin(\beta+\phi) - a_1 \cos(\beta+\phi)\sin\alpha \cos\gamma - a_1 a_2 \sin(\beta+\phi))] \\
& + 2Ia_1 a_2 - 2Ia_2 \cos(\beta+\phi)(-\sin(\beta+\phi)\sin\alpha \cos\gamma + a_1 \cos(\beta+\phi))] \dot{\theta}\dot{\psi} \\
& + [-2mrea_2(-\sin(\beta+\phi)\sin\alpha \cos\gamma + a_1 \cos(\beta+\phi))] \\
& - 2I(\cos(\beta+\phi)\sin\alpha \cos\gamma + a_1 \sin(\beta+\phi))(-\sin(\beta+\phi)\sin\alpha \cos\gamma + a_1 \cos(\beta+\phi))] \dot{\phi}\dot{\psi} \\
& + [2I \cos(\beta+\phi)(-\sin(\beta+\phi)\sin\alpha \cos\gamma + a_1 \cos(\beta+\phi))] \dot{\theta}\dot{\phi} \\
& + [mre - a_1 \cos(\beta+\phi) - Ia_2 \sin(\beta+\phi)\cos(\beta+\phi)]\dot{\theta}^2 \\
& + [mre(\sin(\beta+\phi)\sin\alpha \cos\gamma - a_1 \cos(\beta+\phi))] \dot{\phi}^2 \\
& = 0
\end{aligned} \tag{3.13}$$

where

$$a_1 = -\sin \Theta \sin \gamma + \cos \Theta \cos \alpha \cos \gamma$$

$$a_2 = \cos \Theta \sin \gamma + \sin \Theta \cos \alpha \cos \gamma$$

SPECIALIZATION TO THE CASE OF CONSTANT SHAFT SPEED

The problem is now specialized to the case of constant rotational velocity of the shaft by setting $\ddot{\Psi} = 0$, $\dot{\Psi} = \Omega$, and the equations are put into a nondimensional form by defining the nondimensional parameters,

$$\bar{\rho} = \frac{1}{r} \sqrt{I/m}$$

$$\bar{e} = \frac{e}{r}$$

$$\bar{\omega}_b = \frac{\omega_b}{\Omega} = \frac{1}{\Omega} \sqrt{k_\theta / mr^2}$$

$$\bar{\omega}_t = \frac{\omega_t}{\Omega} = \frac{1}{\Omega} \sqrt{k_\phi / I}$$

and introducing the nondimensional time variable,

$$\tau = \Omega t$$

It is seen that $\bar{\rho}$ is the nondimensional radius of gyration of the mass about the rod axis, \bar{e} is the nondimensional offset of the mass center of gravity from the rod axis and $\bar{\omega}_b$ and $\bar{\omega}_t$ are respectively the nondimensional natural frequencies in restrained bending and restrained torsion when the shaft is not rotating.

Division of Eq. (3.11) by $\Omega^2 mr^2$ and Eq. (3.12) by $\Omega^2 I$ now yields,

$$\begin{aligned}
& [1 + \bar{p}^2 \sin^2(\beta + \phi)] \theta'' + \bar{e} \cos(\beta + \phi) \phi'' \\
& + \left[-2\bar{p}^2 \sin(\beta + \phi) \{ \cos(\beta + \phi) \sin \alpha \cos \gamma + a_1 \sin(\beta + \phi) \} - 2\bar{e} a_2 \sin(\beta + \phi) \right] \phi' \\
& + 2\bar{p}^2 \sin(\beta + \phi) \cos(\beta + \phi) \theta' \phi' - \bar{e} \sin(\beta + \phi) \phi'^2 \\
& + \left[a_1 a_2 + \bar{e} \{ a_1 \cos(\beta + \phi) \sin \alpha \cos \gamma + (a_1^2 - a_2^2) \sin(\beta + \phi) \} \right. \\
& \left. - \bar{p}^2 a_2 \sin(\beta + \phi) \{ \cos(\beta + \phi) \sin \alpha \cos \gamma + a_1 \sin(\beta + \phi) \} \right] \\
& + \bar{\omega}_b^2 \theta = 0 \tag{3.14}
\end{aligned}$$

$$\begin{aligned}
& \ddot{\phi} + \frac{\bar{e}}{\bar{p}^2} \cos(\beta + \phi) \theta'' + \left[2 \frac{\bar{e}}{\bar{p}^2} a_2 \sin(\beta + \phi) \right. \\
& \left. + 2 \sin(\beta + \phi) \{ \cos(\beta + \phi) \sin \alpha \cos \gamma + a_1 \sin(\beta + \phi) \} \right] \theta' \\
& - \sin(\beta + \phi) \cos(\beta + \phi) \theta'^2 + \left[\frac{\bar{e}}{\bar{p}^2} a_2 \{ -\sin(\beta + \phi) \sin \alpha \cos \gamma + a_1 \cos(\beta + \phi) \} \right. \\
& \left. + \{ -\sin(\beta + \phi) \sin \alpha \cos \gamma + a_1 \cos(\beta + \phi) \} \{ \cos(\beta + \phi) \sin \alpha \cos \gamma + a_1 \sin(\beta + \phi) \} \right] \\
& + \bar{\omega}_t^2 \phi = 0 \tag{3.15}
\end{aligned}$$

where primes denote differentiation with respect to τ , and a_1 and a_2 are as defined in the preceding section.

Recognizing that constant shaft speed represents the limiting case of infinite flywheel inertia, the term $I_F \ddot{\psi}$ in Eq. (3.13) can be seen to remain finite and equal to the shaft torque, which may then, from Eq. (3.13), be written in the following nondimensional form,

$$\begin{aligned}
\overline{M}_T = & \left[-\sin \alpha \cos \gamma + \bar{e} a_2 \cos(\beta + \phi) \right. \\
& + \bar{\rho}^2 \sin(\beta + \phi) \{ -\sin(\beta + \phi) \sin \alpha \cos \gamma + a_1 \cos(\beta + \phi) \} \left. \right] \theta'' \\
& + \left[\bar{\rho}^2 a_2 - \bar{e} \{ \cos(\beta + \phi) \sin \alpha \cos \gamma + a_1 \sin(\beta + \phi) \} \right] \phi'' \\
& + \left[-2a_1 a_2 + 2\bar{e} \{ a_2^2 \sin(\beta + \phi) - a_1 \cos(\beta + \phi) \sin \alpha \cos \gamma - a_1 a_2 \sin(\beta + \phi) \} \right. \\
& + 2\bar{\rho}^2 a_1 a_2 - 2\bar{\rho}^2 a_2 \cos(\beta + \phi) \{ -\sin(\beta + \phi) \sin \alpha \cos \gamma + a_1 \cos(\beta + \phi) \} \left. \right] \theta' \\
& + \left[-2\bar{e} a_2 \{ -\sin(\beta + \phi) \sin \alpha \cos \gamma + a_1 \cos(\beta + \phi) \} \right. \\
& - 2\bar{\rho}^2 \{ \cos(\beta + \phi) \sin \alpha \cos \gamma + a_1 \sin(\beta + \phi) \} \{ -\sin(\beta + \phi) \sin \alpha \cos \gamma + a_1 \cos(\beta + \phi) \} \left. \right] \phi' \\
& + 2\bar{\rho}^2 \cos(\beta + \phi) \{ -\sin(\beta + \phi) \sin \alpha \cos \gamma + a_1 \cos(\beta + \phi) \} \theta' \phi' \\
& + [\bar{e} a_1 \cos(\beta + \phi) - \bar{\rho}^2 a_2 \sin(\beta + \phi) \cos(\beta + \phi)] \theta'^2 \\
& + \bar{e} [\sin(\beta + \phi) \sin \alpha \cos \gamma - a_1 \cos(\beta + \phi)] \phi'^2
\end{aligned} \tag{3.16}$$

where

$$\overline{M}_T = \frac{M_T}{m r^2 \Omega^2}$$

and M_T is the dimensional torque.

To facilitate solution, it is desirable to rearrange Eqs. (3.14) and (3.15) in the form,

$$f_1 \theta'' + f_2 \phi'' = -f_3 \theta' \phi' - f_4 \phi' - f_5 \phi'^2 - \bar{\omega}_b^2 \theta - f_6 \tag{3.17}$$

$$f_7 \theta'' + \phi'' = -f_8 \theta' - f_9 \theta'^2 - \bar{\omega}_t^2 \phi - f_{10} \tag{3.18}$$

where

$$\begin{aligned}
f_1 &= 1 + \bar{\rho}^2 \sin^2(\beta + \phi) \\
f_2 &= \bar{e} \cos(\beta + \phi) \\
f_3 &= 2\bar{\rho} \sin(\beta + \phi) \cos(\beta + \phi) \\
f_4 &= -2\bar{\rho}^2 \sin(\beta + \phi) [\cos(\beta + \phi) \sin \alpha \cos \gamma + a_1 \sin(\beta + \phi)] - 2\bar{e} a_2 \sin(\beta + \phi) \\
f_5 &= -\bar{e} \sin(\beta + \phi) \\
f_6 &= a_1 a_2 + \bar{e} \{a_1 \cos(\beta + \phi) \sin \alpha \cos \gamma + (a_1^2 - a_2^2) \sin(\beta + \phi)\} \\
&\quad - \bar{\rho}^2 a_2 \sin(\beta + \phi) [\cos(\beta + \phi) \sin \alpha \cos \gamma + a_1 \sin(\beta + \phi)] \\
f_7 &= \frac{\bar{e}}{\bar{\rho}^2} \cos(\beta + \phi) \\
f_8 &= 2 \frac{\bar{e}}{\bar{\rho}^2} a_2 \sin(\beta + \phi) + 2 \sin(\beta + \phi) [\cos(\beta + \phi) \sin \alpha \cos \gamma + a_1 \sin(\beta + \phi)] \\
f_9 &= -\sin(\beta + \phi) \cos(\beta + \phi) \\
f_{10} &= \frac{\bar{e}}{\bar{\rho}^2} a_2 \{-\sin(\beta + \phi) \sin \alpha \cos \gamma + a_1 \cos(\beta + \phi)\} \\
&\quad + \{-\sin(\beta + \phi) \sin \alpha \cos \gamma + a_1 \cos(\beta + \phi)\} [\cos(\beta + \phi) \sin \alpha \cos \gamma + a_1 \sin(\beta + \phi)]
\end{aligned}$$

Solving Eqs. (3.17) and (3.18) for θ'' and ϕ'' in terms of θ and ϕ and their first derivatives yields the differential equations in the following form,

$$\theta'' = \frac{1}{f_1 - f_2 f_7} [-f_3 \theta' \phi' - f_4 \phi' - f_5 \phi'^2 - \bar{\omega}_b^2 \theta - f_6 + f_2 f_8 \theta' + f_2 f_9 \theta'^2 + f_2 \bar{\omega}_t^2 \phi + f_2 f_{10}] \quad (3.19)$$

$$\begin{aligned}
\phi'' &= \frac{1}{f_1 - f_2 f_7} [-f_1 f_8 \theta' - f_1 f_9 \theta'^2 - f_1 \bar{\omega}_t^2 \phi - f_1 f_{10} + f_7 f_{18} \theta' \phi' \\
&\quad + f_7 f_4 \phi' + f_7 f_5 \phi'^2 + f_7 \bar{\omega}_b^2 \theta + f_7 f_6] \quad (3.20)
\end{aligned}$$

Equations (3.19) and (3.20) are now in suitable form for solution on a digital or analog computer.

SOLUTION OF THE PSEUDO-STATIC PROBLEM

It is of interest to determine the static configuration of the rotating model, that is, the static displacements under the action of centrifugal forces. This problem may be termed the pseudo-static problem. Its solution permits the setting up and solution of linearized differential equations for small motions about the pseudo-static configuration.

The appropriate equations are obtained by eliminating all terms containing derivatives of θ and ϕ from Eqs. (3.17) and (3.18), yielding,

$$\bar{\omega}_b^2 \theta_s + f_{\theta} = 0 \quad (3.21)$$

$$\bar{\omega}_t^2 \phi_s + f_{10} = 0 \quad (3.22)$$

These equations are nonlinear, with f_{θ} and f_{10} being transcendental functions of the dependent variables. Since it is not feasible to obtain an analytical solution in closed form, the following iterative procedure was applied.

Equations (3.21) and (3.22) are linearized with respect to departures $\Delta\theta$ and $\Delta\phi$ from trial values θ_n and ϕ_n , respectively, of the variables, yielding,

$$\bar{\omega}_b^2 \theta_n + \bar{\omega}_b^2 \Delta\theta + f_{\theta n} + \left(\frac{\partial f_{\theta}}{\partial \theta} \right)_n \Delta\theta + \left(\frac{\partial f_{\theta}}{\partial \phi} \right)_n \Delta\phi = 0 \quad (3.23)$$

$$\bar{\omega}_t^2 \phi_n + \bar{\omega}_t^2 \Delta\phi + f_{10n} + \left(\frac{\partial f_{10}}{\partial \theta} \right)_n \Delta\theta + \left(\frac{\partial f_{10}}{\partial \phi} \right)_n \Delta\phi = 0 \quad (3.24)$$

where subscript n denotes values at $\theta = \theta_n$, $\phi = \phi_n$.

Equations (3.23) and (3.24) are now rearranged in the form,

$$(\bar{\omega}_b^2 + f_{11n}) \Delta\theta + f_{12n} \Delta\phi = -f_{\theta n} - \bar{\omega}_b^2 \theta_n \quad (3.25)$$

$$f_{13n} \Delta\theta + (\bar{\omega}_t^2 + f_{14n}) \Delta\phi = -f_{10n} - \bar{\omega}_t^2 \phi_n \quad (3.26)$$

where

$$\begin{aligned}
f_{11} &= \frac{\partial f_6}{\partial \theta} \\
&= a_1^2 - a_2^2 - \bar{e} \{ a_2 \cos(\beta+\phi) \sin \alpha \cos \gamma + 4a_1 a_2 \sin(\beta+\phi) \} \\
&- \bar{p}^2 \sin(\beta+\phi) \{ a_1 \cos(\beta+\phi) \sin \alpha \cos \gamma + (a_1^2 - a_2^2) \sin(\beta+\phi) \}
\end{aligned}$$

$$\begin{aligned}
f_{12} &= \frac{\partial f_6}{\partial \phi} \\
&= \bar{e} \{ -a_1 \sin(\beta+\phi) \sin \alpha \cos \gamma + (a_1^2 - a_2^2) \cos(\beta+\phi) \} \\
&- \bar{p}^2 a_2 \left[\{ \cos^2(\beta+\phi) - \sin^2(\beta+\phi) \} \sin \alpha \cos \gamma + 2a_1 \sin(\beta+\phi) \cos(\beta+\phi) \right]
\end{aligned}$$

$$\begin{aligned}
f_{13} &= \frac{\partial f_{10}}{\partial \theta} \\
&= \frac{\bar{e}}{\bar{p}^2} \{ -a_1 \sin(\beta+\phi) \sin \alpha \cos \gamma + (a_1^2 - a_2^2) \cos(\beta+\phi) \} \\
&- a_2 \left[\{ \cos^2(\beta+\phi) - \sin^2(\beta+\phi) \} \sin \alpha \cos \gamma + 2a_1 \sin(\beta+\phi) \cos(\beta+\phi) \right]
\end{aligned}$$

$$\begin{aligned}
f_{14} &= \frac{\partial f_{10}}{\partial \phi} \\
&= -\frac{\bar{e}}{\bar{p}^2} a_2 \{ \cos(\beta+\phi) \sin \alpha \cos \gamma + a_1 \sin(\beta+\phi) \} \\
&- \{ \cos(\beta+\phi) \sin \alpha \cos \gamma + a_1 \sin(\beta+\phi) \}^2 \\
&+ \{ -\sin(\beta+\phi) \sin \alpha \cos \gamma + a_1 \cos(\beta+\phi) \}^2
\end{aligned}$$

Solution of Eqs. (3.25) and (3.26) for $\Delta\theta$ and $\Delta\phi$ yields,

$$\Delta\theta = \frac{-e_{4n}e_{2n} + e_{5n}f_{12n}}{e_{3n}} \quad (3.27)$$

$$\Delta\phi = \frac{-e_{5n}e_{1n} + e_{4n}f_{13n}}{e_{3n}} \quad (3.28)$$

where

$$e_1 = \bar{\omega}_b^2 + f_{11}$$

$$e_2 = \bar{\omega}_t^2 + f_{14}$$

$$e_3 = e_1 e_2 - f_{12} f_{13}$$

$$e_4 = \bar{\omega}_b^2 \theta_n + f_6$$

$$e_5 = \bar{\omega}_t^2 \phi_n + f_{10} .$$

Equations (3.27) and (3.28) may be applied in conjunction with the iteration formulae,

$$\theta_{n+1} = \theta_n + \Delta\theta \quad (3.29)$$

$$\phi_{n+1} = \phi_n + \Delta\phi \quad (3.30)$$

using as initial values, $\theta_1 = 0$, $\phi_1 = 0$. The process has been found to converge rapidly in the cases that have been considered in the present work.

FORMULATION AND SOLUTION OF THE LINEARIZED EQUATIONS

In order to assess the significance of nonlinear effects in the problem under consideration, it is desirable to obtain also solutions to linearized equations for small perturbations $\bar{\theta}$ and $\bar{\phi}$ from the pseudo-static configuration.

Application of small perturbation theory to Eqs. (3.17) and (3.18) yields,

$$f_{1s} \bar{\theta}'' + (\bar{\omega}_b^2 + f_{11s}) \bar{\theta} + f_{2s} \bar{\phi}'' + f_{4s} \bar{\phi}' + f_{12s} \bar{\phi} = 0 \quad (3.31)$$

$$f_{7s} \bar{\theta}'' + f_{8s} \bar{\theta}' + f_{13s} \bar{\theta} + \bar{\phi}'' + (\bar{\omega}_t^2 + f_{14s}) \bar{\phi} = 0 \quad (3.32)$$

in which subscript s denotes values corresponding to the pseudo-static configuration $\theta = \theta_s$, $\phi = \phi_s$.

Putting Eqs. (3.31) and (3.32) into operator form, using symbol p to denote the differential operator, and expanding the determinant of coefficients,

the following characteristic equation is obtained,

$$c_1 p^4 + c_2 p^2 + c_3 = 0 \quad (3.33)$$

where

$$c_1 = f_{1s} - f_{2s} f_{7s}$$

$$c_2 = f_{1s}(\bar{\omega}_t^2 + f_{14s}) + \bar{\omega}_b^2 + f_{11s} - f_{2s} f_{13s} - f_{7s} f_{12s} - f_{4s} f_{8s}$$

$$c_3 = (\bar{\omega}_b^2 + f_{11s})(\bar{\omega}_t^2 + f_{14s}) - f_{12s} f_{13s} .$$

The terms in p and p^3 are seen to vanish.

The roots of this equation are

$$p_1^2 = \frac{1}{2c_1} (-c_2 + \sqrt{c_2^2 - 4c_1 c_3})$$

$$p_2^2 = \frac{1}{2c_1} (-c_2 - \sqrt{c_2^2 - 4c_1 c_3})$$

and the characteristic frequencies are given by

$$\bar{\omega}_1 = \sqrt{-p_1^2} \quad (3.34)$$

$$\bar{\omega}_2 = \sqrt{-p_2^2} . \quad (3.35)$$

The characteristic mode shapes may be determined by assuming a solution of the form,

$$\bar{\theta} = \bar{\theta}_0 \cos \bar{\omega} \tau \quad (3.36)$$

$$\bar{\phi} = \bar{\phi}_0 \cos \bar{\omega} \tau + \frac{\bar{\phi}'_0}{\bar{\omega}} \sin \bar{\omega} \tau = \bar{\phi}_1 \cos (\bar{\omega} \tau - \epsilon) . \quad (3.37)$$

introducing Eqs. (3.36) and (3.37) into Eq. (3.31), and equating the sum of the coefficients of the $\cos \bar{\omega}\tau$ and the $\sin \bar{\omega}\tau$ terms respectively to zero, the following result is obtained,

$$\bar{\phi}_0/\bar{\theta}_0 = \frac{(f_{2s}\bar{\omega}^2 - f_{12s})(-f_{1s}\bar{\omega}^2 + \bar{\omega}_0^2 + f_{11s})}{(f_{2s}\bar{\omega}^2 - f_{12s})^2 + f_{4s}^2\bar{\omega}^2} \quad (3.38)$$

$$\bar{\phi}'_0/\bar{\theta}_0 = - \frac{f_{4s}\bar{\omega}^2(-f_{1s}\bar{\omega}^2 + \bar{\omega}_0^2 + f_{11s})}{(f_{2s}\bar{\omega}^2 - f_{12s})^2 + f_{4s}^2\bar{\omega}^2} \quad (3.39)$$

where $\bar{\omega} = \bar{\omega}_1, \bar{\omega}_2$.

The mode shapes may be expressed alternatively in the form,

$$\bar{\phi}_1/\bar{\theta}_0 = \left\{ \left(\frac{\bar{\phi}_0}{\bar{\theta}_0} \right)^2 + \left(\frac{\bar{\phi}'_0}{\bar{\omega}\bar{\theta}_0} \right)^2 \right\}^{1/2} \quad (3.40)$$

$$\epsilon = \tan^{-1} \left(\frac{\bar{\phi}'_0}{\bar{\omega}\bar{\phi}_0} \right) \quad (3.41)$$

where, from Eq. (3.37) it is seen that $\bar{\phi}_1/\bar{\theta}_0$ is the relative amplitude of displacements in the two coordinates and ϵ is the phase lag of the oscillation in the ϕ -coordinate relative to that in the θ -coordinate.

A solution involving only one characteristic mode of oscillation may be obtained by selecting as initial conditions,

$$\theta = \theta_s + \bar{\theta}_0, \quad \phi = \phi_s + \bar{\phi}_0, \quad \phi' = \bar{\phi}'_0 \quad (3.42)$$

where $\bar{\theta}_0$ may be selected arbitrarily within the limitations imposed by the assumption of small perturbations, and $\bar{\phi}_0$ and $\bar{\phi}'_0$ are then determined from Eqs. (3.38) and (3.39).

It should be noted that the existence of a phase difference between oscillation in the two coordinates is associated with the presence of the terms $f_{4s}\bar{\phi}'$ and $f_{8s}\bar{\theta}'$ in Eqs. (3.31) and (3.32) respectively. These terms originate in the terms in $\dot{\theta}\psi$ and $\dot{\phi}\psi$ in Eqs. (3.11) and (3.12), which are due to the presence of Coriolis forces.

DISCUSSION OF RESULTS

A series of computations on the simple model were performed using an auto-

matic digital computer. These computations were limited to the case of constant rotational velocity of the shaft and zero built-in coning angle ($\gamma = 0$).

The pseudo-static configuration was determined by means of the iterative procedure developed earlier, and corresponding characteristics of the linearized system for small perturbations from this configuration were computed. In each case additional computations were performed in which the terms $f_{4s}\bar{\phi}'$ and $f_{8s}\bar{\theta}'$ in Eqs. (3.31) and (3.32) were omitted. As discussed previously, these terms represent the influence of Coriolis forces, so that a comparison of results obtained with and without their inclusion provides a means of assessing the importance of the Coriolis forces.

These results are presented in Figs. 3.2 to 3.8 inclusive. Figures 3.2 and 3.3 show the effect of varying the mass offset parameter \bar{e} , with the parameter $\bar{\rho}_0$, representing the nondimensional radius of gyration of the mass about its center of gravity, and the parameters, α , β , $\bar{\omega}_b$ and $\bar{\omega}_t$ being maintained constant. Since the parameter \bar{p} must be varied accordingly, the maintenance of a constant value for $\bar{\omega}_t$ implies that the variation of \bar{e} does not involve merely a shifting of the mass relative to the supporting arm but involves also changes in m or $k\phi$ or both. The value of $\bar{\rho}_0$ selected for this case represents a rather extreme value, applicable to a short, wide blade.

Figure 3.2 shows the substantial pseudo-static deformation occurring in

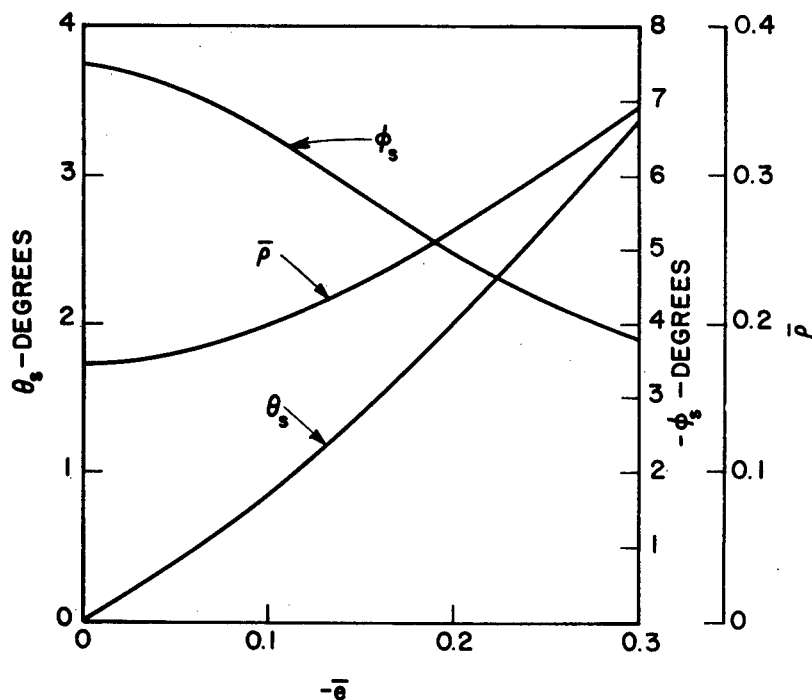


Fig. 3.2. Effect of mass offset on pseudo-static displacements of model. $\alpha = 30^\circ$, $\beta = 15^\circ$, $\bar{\omega}_b = 1/3$, $\bar{\omega}_t = 1$, $\bar{\rho}_0 = 0.1732$.

this case. It should be noted that the static twist decreases with increase in offset, when the center of gravity of the mass is behind the elastic axis. This occurs despite the fact that the relative values of the moment of inertia and torsional stiffness about the supporting arm remain the same because of the constancy of $\bar{\omega}_t$, which fact implies that centrifugal twisting moment, before deformation, remains the same. It must be concluded that the variation in twist is associated with a component of centrifugal force normal to the coning surface on which the supporting arm revolves. This effect is introduced through the term in $mre\dot{\psi}^2$ in Eq. (3.12) and terms deriving from it in later forms. It has been called "centrifugal force coupling" in Ref. 2, and shown there to have a substantial effect on natural coupled frequencies of vibration. In the present case, since $\gamma = 0$, the coning of the supporting arm is associated solely with the displacement θ_s . With positive θ_s and a positive value for $(\alpha + \beta + \phi_s)$, this effect opposes that of centrifugal twisting moment. It can be expected to be more pronounced in the case of blades with built-in coning angle.

Figure 3.3 shows the effect of mass offset on the natural vibration characteristics of the system linearized with respect to the pseudo-static configuration. As can be expected, it is seen that the increased coupling between bending and torsion associated with increasing mass offset separates the natural frequencies and alters the natural mode shapes.

It is seen also that the Coriolis forces introduce substantial phase differences between motion in the two coordinates, particularly in the case of the first or predominantly bending mode, where the phase angle is large throughout the range of \bar{e} considered. In the case of the second mode, where torsional motion predominates, the phase angle is substantial only at small values of \bar{e} . When \bar{e} is zero the only coupling between bending and torsion is through the Coriolis forces, and the phase difference is then 90° , $\bar{\phi}$ leading $\bar{\theta}$ by this amount in the case of the first mode and lagging by this amount in the case of the second mode. Furthermore, the Coriolis forces are seen to have a substantial effect on the mode shape of the first mode and a somewhat modest effect on the corresponding frequency. The corresponding effects on the second mode and frequency are seen to be small or negligible. It should be noted here that the apparent absence in some cases of curves associated with neglect of Coriolis forces is explained by the fact that such curves are indistinguishable from the corresponding solid-line curves, and the effect of these forces is thus very small.

Figures 3.4 and 3.5 provide results corresponding to those of Figs. 3.2 and 3.3 for a different case, namely one involving a much smaller value of \bar{p}_0 and consequently more realistic in relation to propeller or helicopter rotor blades. Similar trends are observed, except that Coriolis force effects are considerably reduced, but still substantial with respect to phase differences in the first mode.

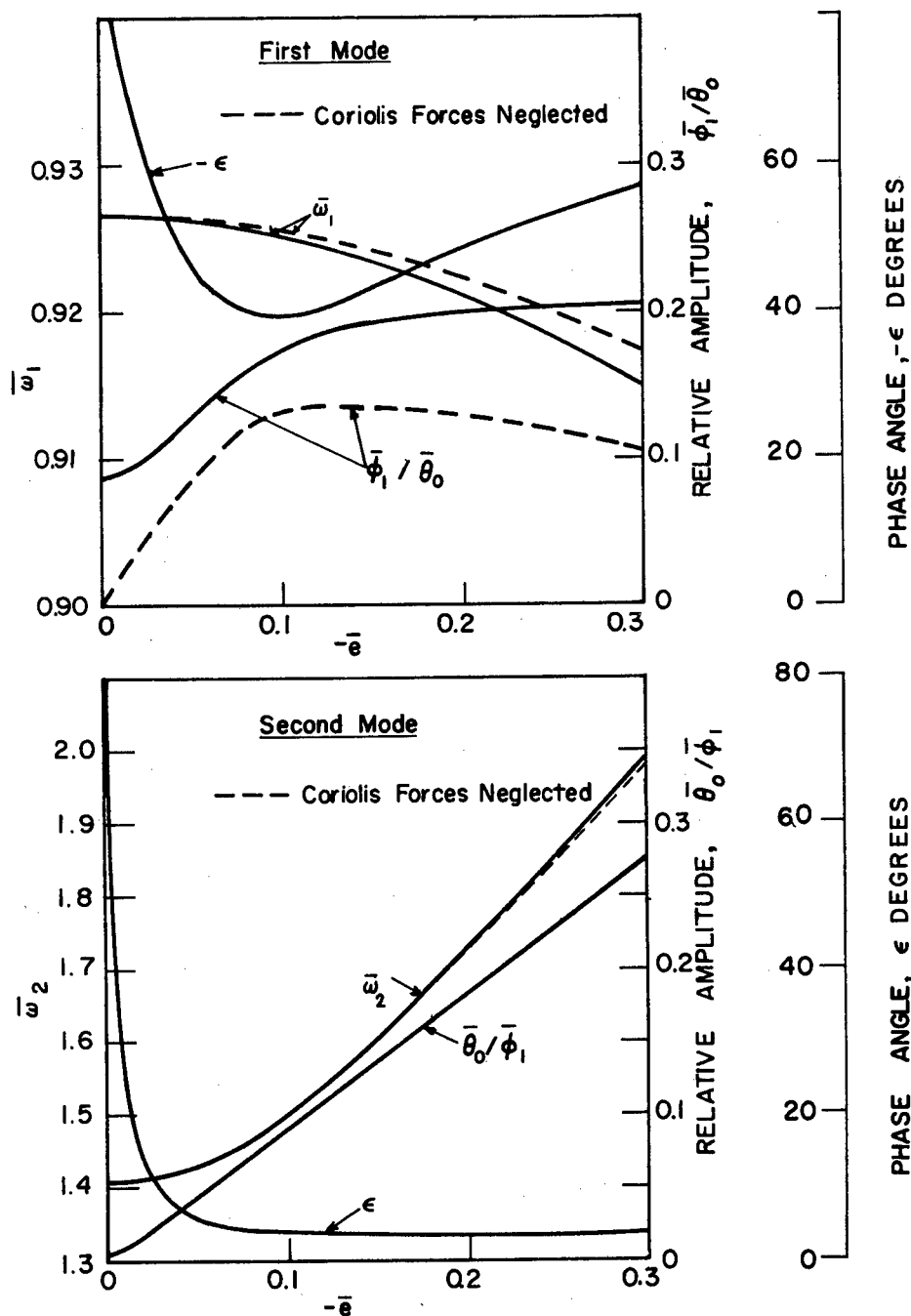


Fig. 3.3. Effect of mass offset on natural vibration characteristics of model. $\alpha = 30^\circ$, $\beta = -15^\circ$, $\bar{\omega}_b = 1/3$, $\bar{\omega}_t = 1$, $\bar{\rho}_0 = 0.1732$.

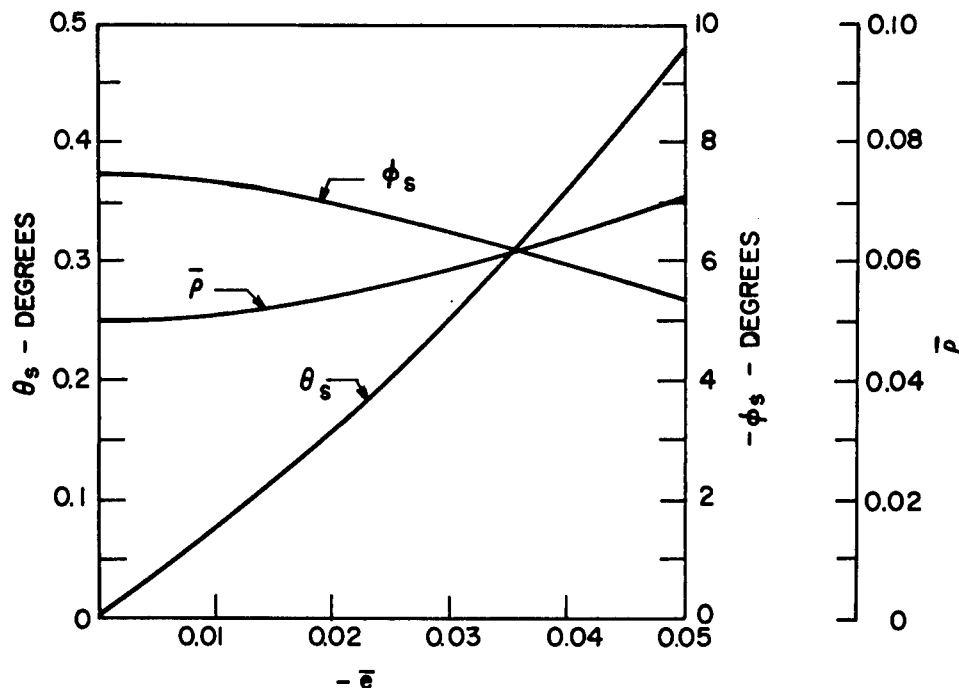


Fig. 3.4. Effect of mass offset on pseudo-static displacements of model. $\alpha = 30^\circ$, $\beta = -15^\circ$, $\bar{\omega}_b = 1/3$, $\bar{\omega}_t = 1$, $\bar{\rho}_0 = 0.05$.

Figure 3.6 shows the effect of varying the bending hinge orientation angle while maintaining the orientation of the principal axis of the mass fixed. This involves varying α and β so that $\alpha + \beta$ remains constant, and simulates a situation in which mean blade angle is kept constant while built-in twist is varied. All other parameters were maintained constant. Curves of θ_s and ϕ_s are not shown, as variations in those parameters were small. For a variation of α from 15° to 45° , θ_s varied from 0.78° to 0.97° and ϕ_s varied from -6.50° to -6.60° . It is seen from Fig. 3.6 that first mode characteristics are affected very substantially by changes in α , the phase difference between the $\bar{\theta}$ and $\bar{\phi}$ motions especially varying over a very wide range. The effect on second mode characteristics is much smaller, although still considerable.

Figures 3.7 and 3.8 show the effect of varying the rotational velocity of the shaft while other parameters remain constant. The information in Fig. 3.7 is principally of value in estimating the pseudo-static torsional deformation corresponding to a given rotational velocity. This deformation can be expected to depend primarily on the parameter $\bar{\omega}_t$ in the case of a blade without built-in coning angle, although from results discussed earlier it can be seen also to depend somewhat on the parameters \bar{e} and $\bar{\omega}_b$. From Fig. 3.7 it can be seen that

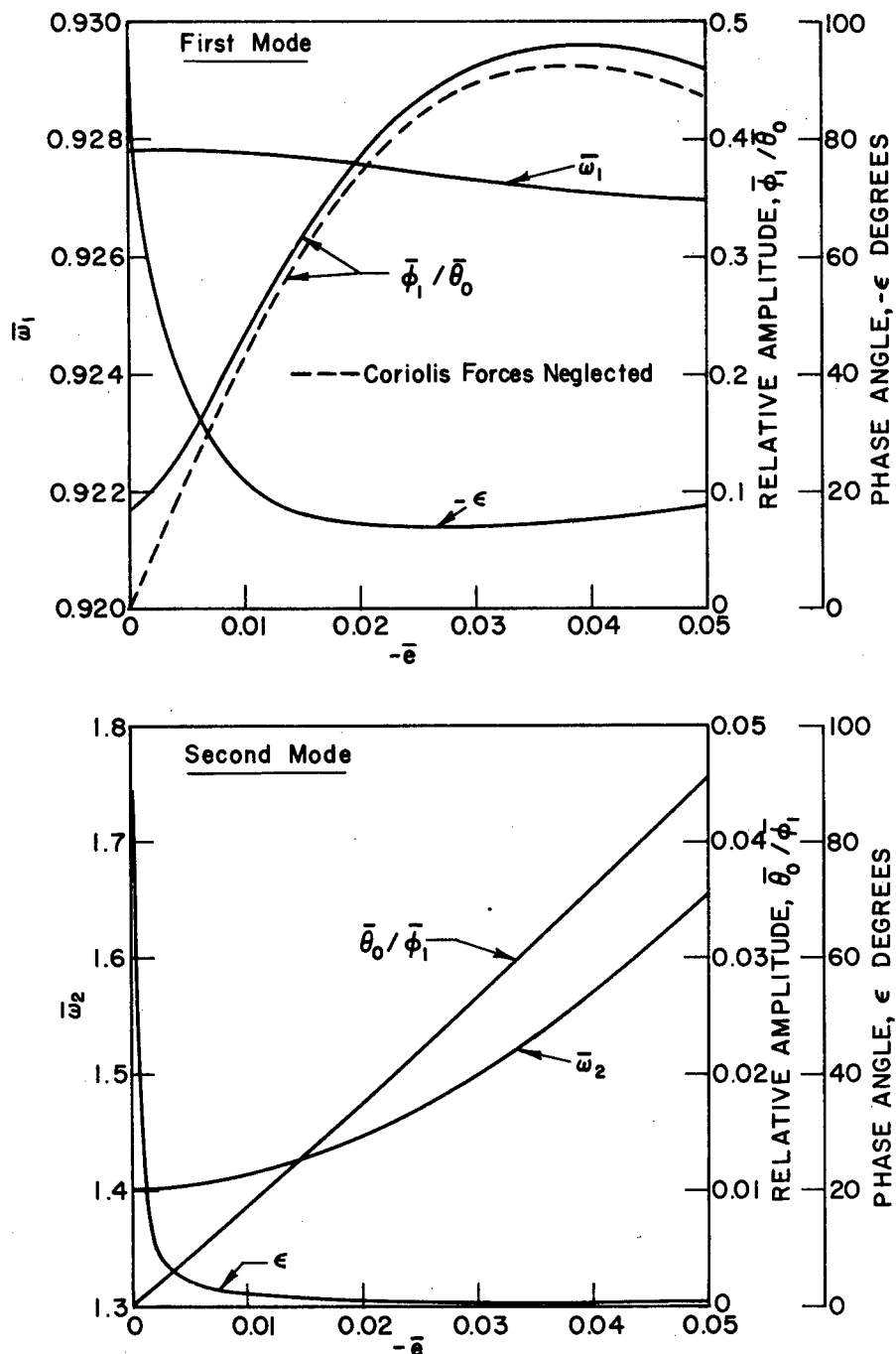


Fig. 3.5. Effect of mass offset on natural vibration characteristics of model. $\alpha = 30^\circ$, $\beta = -15^\circ$, $\bar{\omega}_b = 1/3$, $\bar{\omega}_t = 1$, $\bar{\rho}_0 = 0.05$.

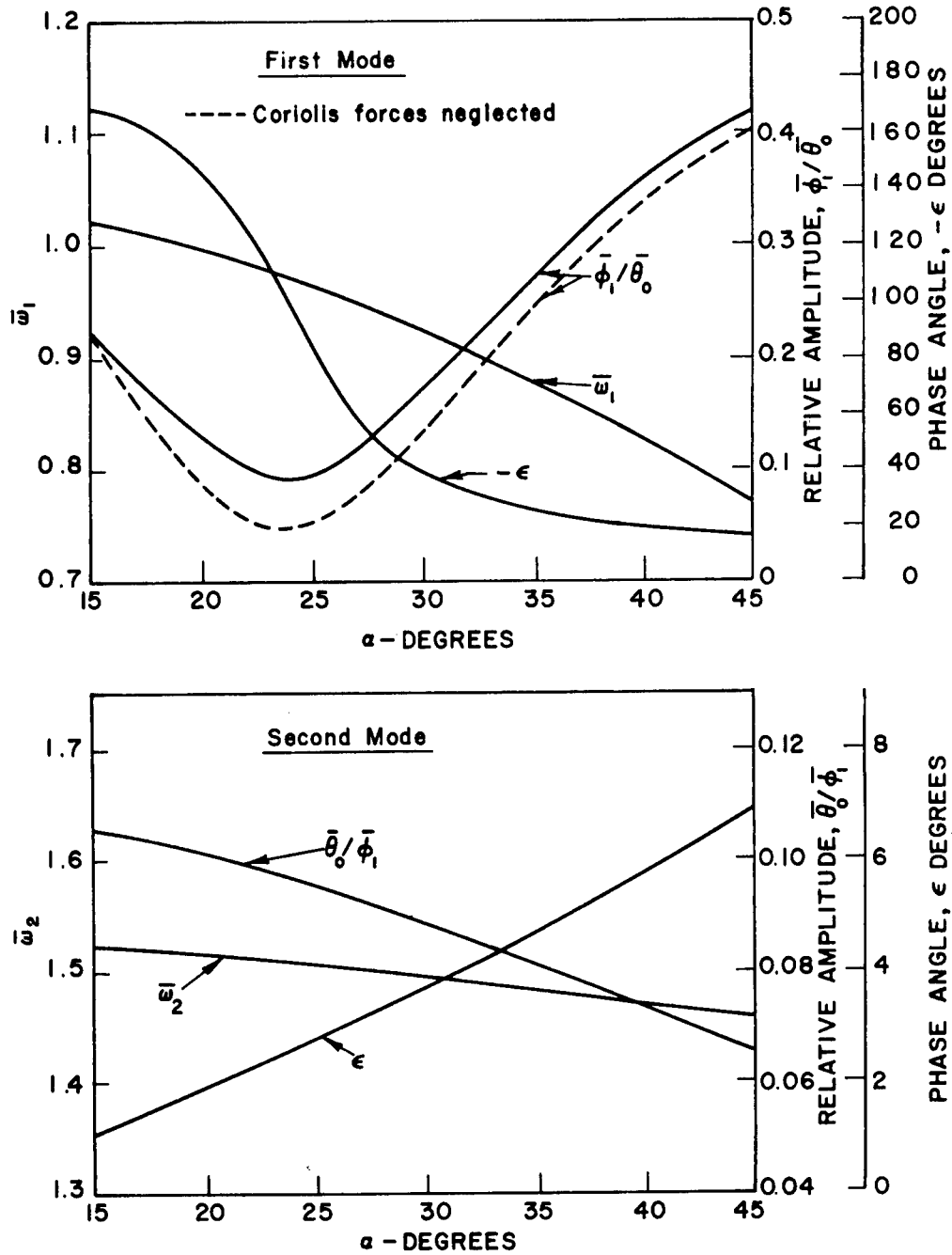


Fig. 3.6. Effect of bending hinge orientation on natural vibration characteristics of model. $\alpha + \beta = 15^\circ$, $\bar{\omega}_b = 1/3$, $\bar{\omega}_t = 1$, $\rho = 0.2$, $\bar{e} = -0.1$.

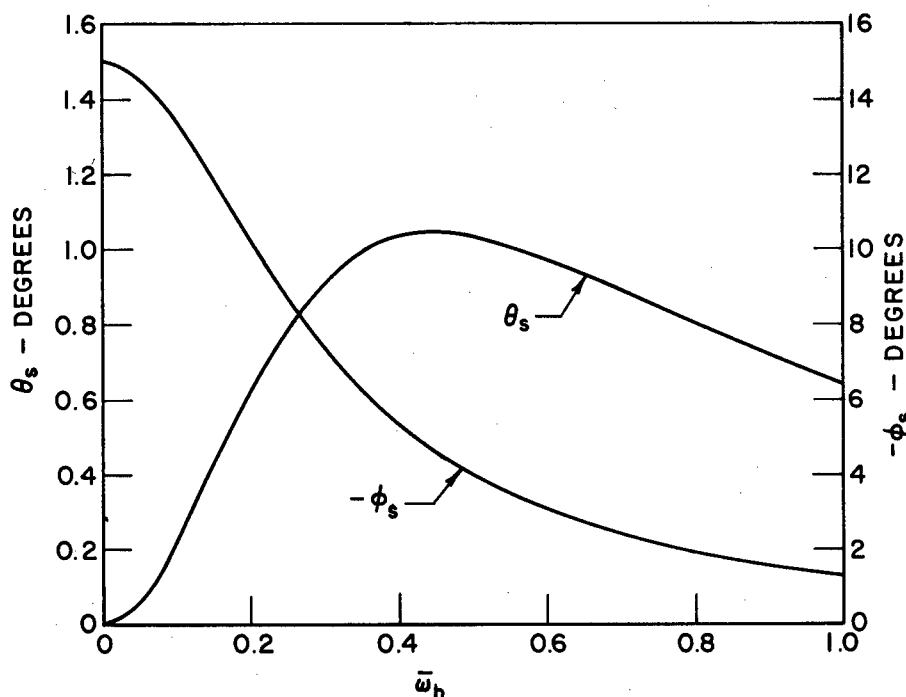


Fig. 3.7. Effect of rotational velocity on pseudo-static displacements of model. $\bar{\omega}_t/\bar{\omega}_b = 3$, $\alpha = 45^\circ$, $\beta = -15^\circ$, $\bar{\rho} = 0.2$, $\bar{e} = -0.1$.

the torsional displacement will exceed 20% of the initial blade angle ($\alpha + \beta$) if $\bar{\omega}_t$ is less than about 2, that is, if the rotational velocity is greater than about one-half the value of restrained torsional frequency corresponding to zero rotational velocity.

Figure 3.8 indicates an increasing prominence of torsion relative to bending in both modes as rotational velocity becomes large. It indicates further a marked sensitivity of the phase difference between coordinates in the first mode to variation in rotational velocity, at least in a limited range of rotational velocity. The phase angle is seen to approach zero at large values of rotational velocity. A somewhat different situation is seen to exist in the case of the second mode, where the phase angle increases with increase in rotational velocity.

Digital computer solutions to the nonlinear differential equations were also obtained, using a Runge-Kutta procedure. Initial conditions were established on the basis of natural vibration characteristics determined from the linearized equations, that is, by applying Eqs. (3.42), using values from Eqs. (3.38) and (3.39) and the pseudo-static displacements. With such initial con-

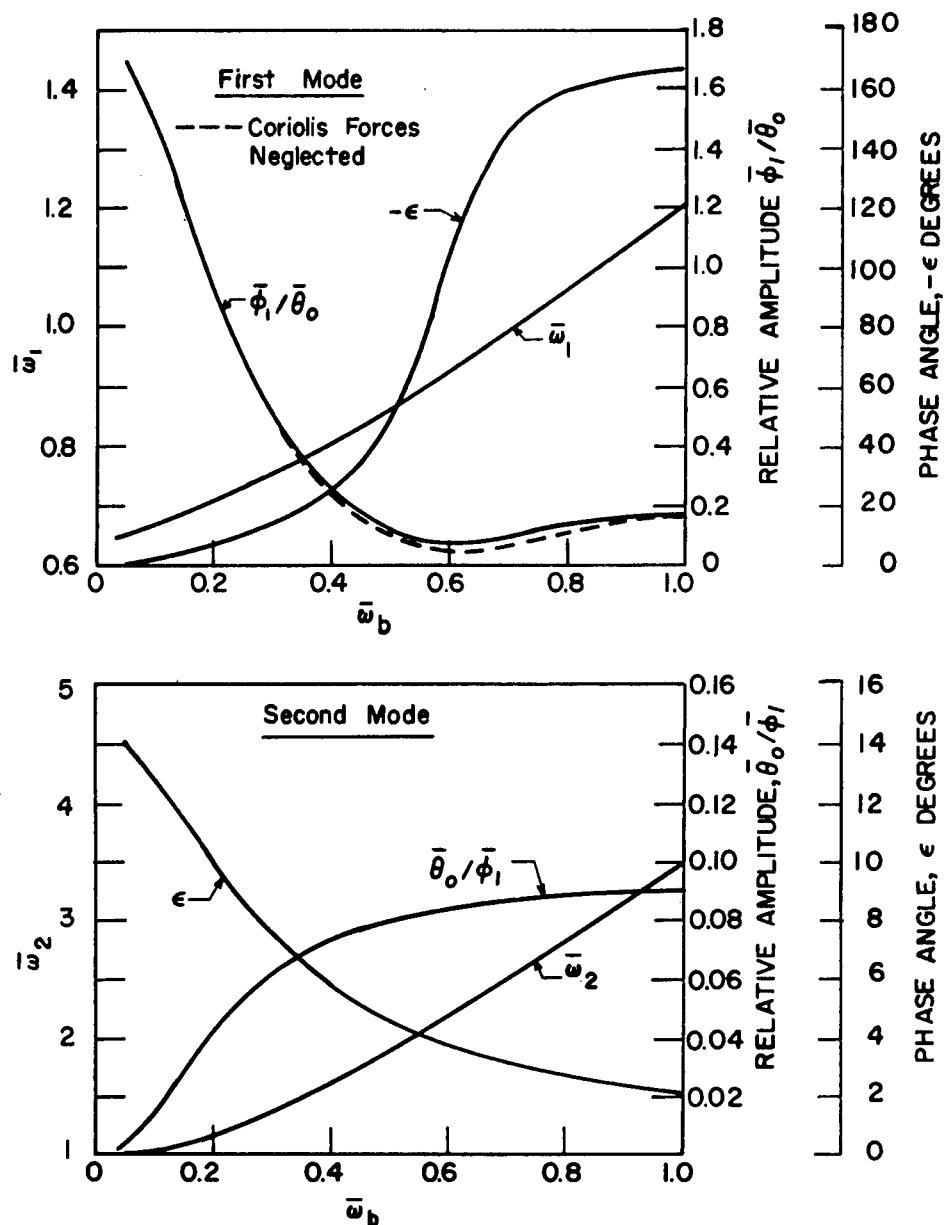


Fig. 3.8. Effect of rotational velocity on natural vibration characteristics of model. $\bar{\omega}_t/\bar{\omega}_b = 3$, $\alpha = 45^\circ$, $\beta = -15^\circ$, $\bar{\rho} = 0.2$, $\bar{e} = -0.1$.

ditions, the linearized system responds in only one of the natural modes, and comparison with the corresponding response of the nonlinear system provides a means of assessing the extent to which nonlinear effects distort the motion.

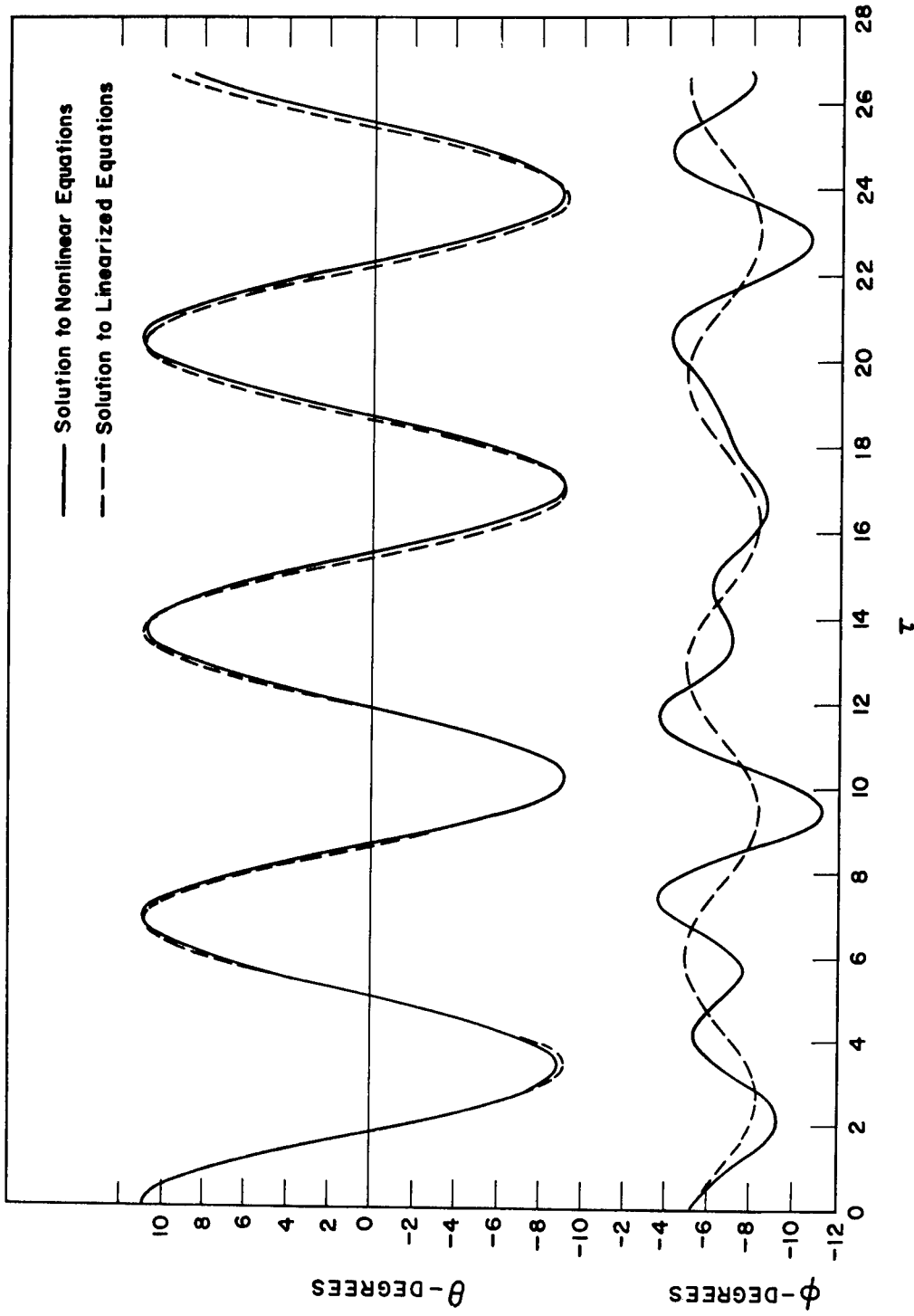
Results were obtained for only one case and are shown in Fig. 3.9. Figure 3.9(a) illustrates the response of the first mode when the initial bending displacement from the pseudo-static configuration is 10° . Displacement in the bending coordinate predominates in that mode and its time history is seen to be distorted only slightly by nonlinear effects. There is a slight increase in period and a very slight but irregular variation in amplitude. The torsional response is seen to be strongly influenced by nonlinear effects in a manner which suggests that there is substantial coupling with the second mode. The slight variation in amplitude of the bending motion is likely associated with this coupling.

The response in the second mode for an initial bending displacement of 2° from the pseudo-static configuration is shown in Fig. 3.9(b). In this case, displacement in the torsional coordinate predominates and has an amplitude of about 22.5° . It is seen that there is an appreciable increase in period caused by nonlinear effects, but otherwise only a slight distortion of the motion in both coordinates. Again, it is likely that this distortion is due to coupling with the first mode.

The solutions were not carried far enough to ascertain whether there is a decay or divergence of the oscillations. The fact that such may exist is not inconceivable, in view of the fact that the system is not necessarily conservative. It has been seen to be conservative when linearized with respect to small perturbations from the pseudo-static configuration. However, with imposition of the condition of constant shaft rotational velocity it is a driven system, and it is possible that nonlinear effects may result in a transfer of energy to or from it through the shaft.

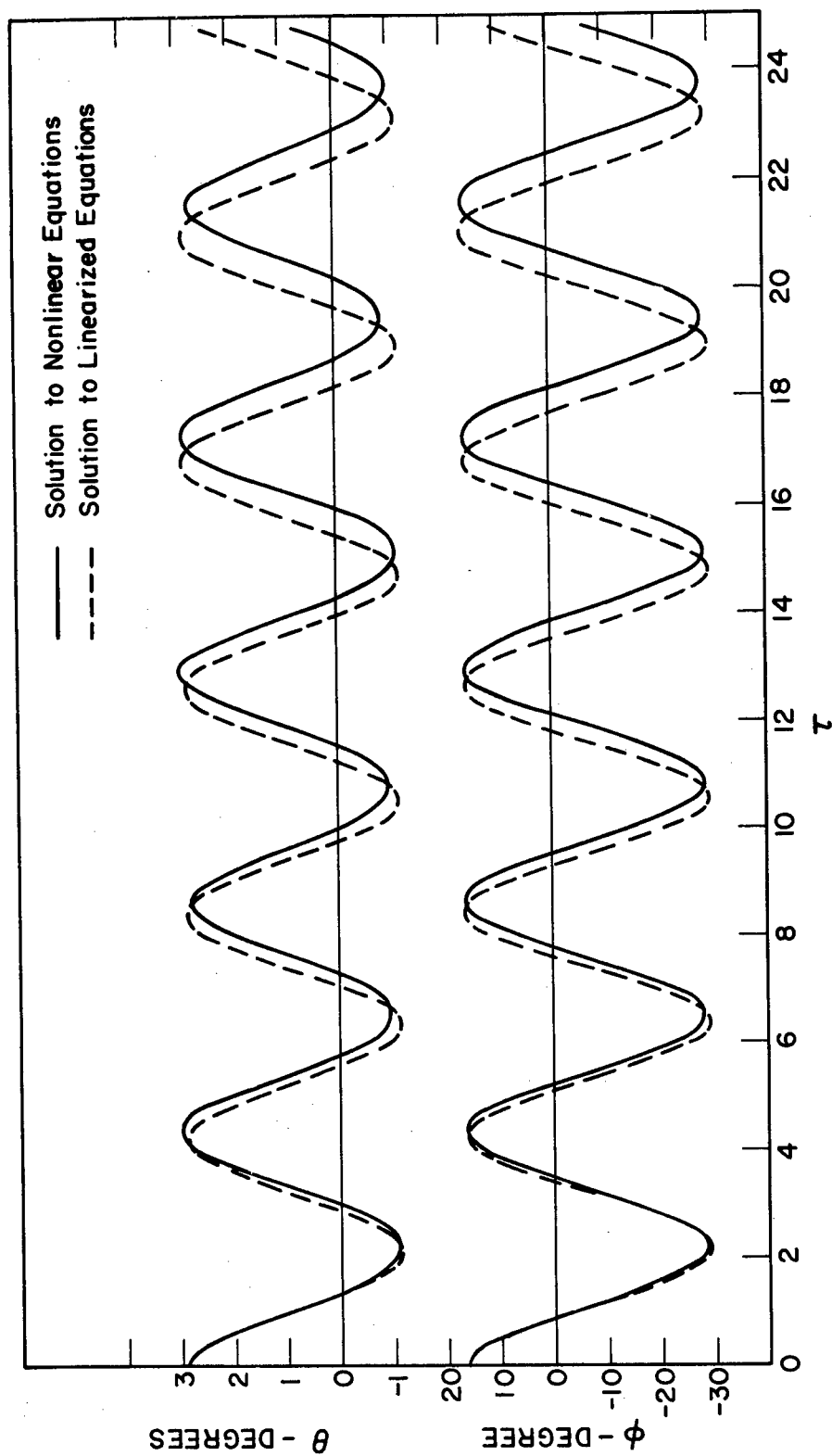
The results obtained indicate that, at least for the case considered, any such divergence or decay will be small and probably represent a negligible effect in comparison with aerodynamic effects in the case of an actual blade. It is possible that a different choice of parameters or the introduction of built-in coning may produce a different result. This requires further investigation.

On the basis of the present results it appears that the effect of Coriolis forces is likely to have a greater practical significance than the effect of nonlinearity, particularly since it does not depend upon the existence of large motions. This relates mainly to the problem of blade flutter, since the flutter phenomenon is highly sensitive to phase differences between motion in bending and torsion. The phase differences associated with the presence of Coriolis forces may conceivably alter the balance in the flutter problem sufficiently to change the conditions for flutter significantly.



(a) INITIAL CONDITIONS APPROPRIATE TO FIRST MODE RESPONSE

Fig. 3.9. Response of model as determined by nonlinear and linearized differential equations. $\alpha = 30^\circ$, $\beta = -15^\circ$, $\bar{\omega}_b = 1/3$, $\bar{\omega}_t = 1$, $\bar{\rho} = 0.2$, $\bar{e} = -0.1$.



(b) INITIAL CONDITIONS APPROPRIATE TO SECOND MODE RESPONSE

Fig. 3.9. Concluded.

Other effects which have not been considered in the present study, but which can be expected to be of considerable importance in some cases, are those of nonlinearity of the torsional spring and of centrifugal tension on torsional stiffness and on pseudo-static deformation, as discussed in the Introduction. Their introduction into the present analysis should not result in undue complication and would represent an appropriate and desirable extension of the present work.

4. CONCLUDING REMARKS

A practical numerical method, suitable for implementation on an automatic digital computer, has been developed for determining the natural vibration characteristics of twisted rotating and nonrotating blades in coupled bending and torsion. A limited numerical study indicates that the method is an efficient one for including the effects of bending-torsion coupling and pre-twist. The nature of the coupling is complicated and a much more extensive parametric study would be needed in order to draw general conclusions. It can be said, however, that centrifugal force coupling can have an appreciable effect when there is a substantial offset of the mass axis from the elastic axis.

In order to investigate some effects of nonlinearity and Coriolis forces in the rotating blade vibration problem, a study has been made of a simple model with a small number of degrees of freedom. Computations performed on this model indicate the following:

(1) There is an effect of centrifugal force, apart from the familiar centrifugal twisting moment, on the torsional deformation when the mass axis of the blade is offset from the elastic axis. It may, in some cases, modify the static deformation of the rotating blade substantially, and tends to introduce additional coupling between bending and torsion when the blade is vibrating, as discussed also in the case of the continuous blade.

(2) The presence of Coriolis forces causes a phase difference between the bending and torsional oscillations which is equal to 90° when the mass and elastic axes are coincident. This phase difference decreases when the mass and elastic axes are not coincident, but remains substantial in the case of a natural mode of the model consisting primarily of bending.

(3) Nonlinear effects for large motions tend to change the natural frequencies of the system slightly and introduce some coupling between the natural vibration modes associated with solution of the linearized equations. A limited amount of results did not provide any evidence of decay or divergence of the free vibrations of the model.

APPENDIX A

DIFFERENTIAL EQUATIONS OF MOTION

The differential equations for free motion of a rotating twisted blade with offset mass and elastic axes are, from Ref. 2, with some changes in notation,

$$\begin{aligned}
 & - \left\{ [GJ_e + Tk_A^2 + EB_1(\beta')^2] \phi' - EB_2 \beta' (\delta_y'' \cos \beta + \delta_z'' \sin \beta) \right\}' \\
 & + Te_A (\delta_y'' \sin \beta - \delta_z'' \cos \beta) + \Omega^2 \rho x e (-\delta_y' \sin \beta + \delta_z' \cos \beta) \\
 & + \Omega^2 \rho e (\sin \beta) \delta_y + \Omega^2 \rho [(k_\xi^2 - k_\eta^2) \cos 2\beta + e e_0 \cos \beta] \phi' \\
 & + \rho (k_\xi^2 + k_\eta^2) \phi'' - \rho e (\delta_y'' \sin \beta - \delta_z'' \cos \beta) = + (Tk_A^2 \beta')' \\
 & - \Omega^2 \rho [(k_\xi^2 - k_\eta^2) \sin \beta \cos \beta + e e_0 \sin \beta] \\
 & \left[(EI_1 \cos^2 \beta + EI_2 \sin^2 \beta) \delta_z'' + (EI_2 - EI_1) \sin \beta (\cos \beta) \delta_y'' \right. \\
 & \left. - Te_A \phi \cos \beta - EB_2 \beta' \phi' \sin \beta \right]'' - (T \delta_z')' - (\Omega^2 \rho x e \phi \cos \beta)' \\
 & + \rho (\delta_z'' + e \phi'' \cos \beta) = (Te_A \sin \beta)'' + (\Omega^2 \rho x e \sin \beta)' \quad (A1) \\
 & + \rho (\delta_z'' + e \phi'' \cos \beta) = (Te_A \sin \beta)'' + (\Omega^2 \rho x e \sin \beta)' \\
 & \left[(EI_2 - EI_1) \sin \beta (\cos \beta) \delta_z'' + (EI_1 \sin^2 \beta + EI_2 \cos^2 \beta) \delta_y'' \right. \\
 & \left. + Te_A \phi \sin \beta - EB_2 \beta' \phi' \cos \beta \right]'' - (T \delta_y')' + (\Omega^2 \rho x e \phi \sin \beta)' \\
 & + \Omega^2 \rho e \phi \sin \beta + \rho (\delta_y'' - e \phi'' \sin \beta) - \Omega^2 \rho \delta_y = + (Te_A \cos \beta)'' \\
 & + (\Omega^2 \rho x e \cos \beta)' + \Omega^2 \rho (e_0 + e \cos \beta)
 \end{aligned}$$

An explanation of the origin of the various terms in the equations is given in Ref. 2. The integrals which define the section constants B_1 and B_2

are given below

$$\begin{aligned} B_1 &= \int_A (\eta^2 + \zeta^2 - k_A^2)(\eta^2 + \zeta^2) dA \\ B_2 &= \int_A (\eta^2 + \zeta^2 - k_A^2) \eta dA \end{aligned} \tag{A2}$$

All other symbols are defined in the list of symbols. The coordinate system is as shown in Fig. 2.1.

It should be noted that Eqs. (A1) are for small displacements from the undeformed configuration of the blade when it is not rotating. The analysis of the present report linearizes the problem with respect to small displacements from the steady-state deformed configuration of the rotating blade.

APPENDIX B

RESULTANT LOADINGS

The resultant loadings per unit length in the x, ζ , and η directions have been obtained in Ref. 2 for a rotating twisted blade with offset mass and elastic axes. The loads include the inertial, centrifugal and Coriolis force terms. In the notation of the present report they are

$$\begin{aligned}
 p_x &= -\rho(\ddot{u} - \Omega^2 u) - 2\Omega\rho\dot{\delta}_1 \sin \beta + 2\Omega\rho\dot{\delta}_2 \cos \beta \\
 &\quad - \rho e\ddot{\delta}_1\beta' + \rho e\ddot{\delta}_2' + \Omega^2 \rho e\delta_1\beta' - \Omega^2 \rho e\delta_2' - 2\Omega\rho e\dot{\beta} \sin \beta + \Omega^2 \rho x \\
 p_\eta &= -\rho\ddot{\delta}_2 + \Omega^2 \rho(-\delta_1 \sin \beta \cos \beta + \delta_2 \cos^2 \beta + e_0 \cos \beta) \\
 &\quad - 2\Omega\rho\dot{u} \cos \beta + \Omega^2 \rho e \cos^2 \beta - \Omega^2 \rho e\dot{\beta} \sin \beta \cos \beta \\
 &\quad - \Omega^2 \rho e_0\dot{\beta} \sin \beta - \Omega^2 \rho e\dot{\beta} \sin \beta \cos \beta + 2\Omega\rho e \cos \beta(-\dot{\delta}_1\beta' + \dot{\delta}_2') \\
 p_\zeta &= -\rho\ddot{\delta}_1 - \Omega^2 \rho(-\delta_1 \sin^2 \beta + \delta_2 \sin \beta \cos \beta + e_0 \sin \beta) + 2\Omega\rho\dot{u} \sin \beta \\
 &\quad - \rho e\ddot{\beta} - \Omega^2 \rho e \sin \beta \cos \beta + \Omega^2 \rho e\dot{\beta} \sin^2 \beta - 2\Omega\rho e \sin \beta(-\dot{\delta}_1\beta' + \dot{\delta}_2') \\
 &\quad - \Omega^2 \rho e_0\dot{\beta} \cos \beta - \Omega^2 \rho e\dot{\beta} \cos^2 \beta \tag{B1} \\
 q_x &= -\Omega^2 \rho e [(-\delta_1 \sin \beta + \delta_2 \cos \beta + e_0) \sin \beta + e_0\dot{\beta} \cos \beta] \\
 &\quad + \rho e(-\ddot{\delta}_1 + 2\Omega\dot{u} \sin \beta) - \Omega^2 [(I_\zeta - I_\eta) \sin \beta \cos \beta + (I_\zeta - I_\eta)\dot{\beta} \cos 2\beta] \\
 &\quad - (I_\zeta + I_\eta)\ddot{\beta} - 2\Omega(I_\zeta - I_\eta)(-\dot{\delta}_1' \sin \beta - \dot{\delta}_1\beta' \cos \beta + \dot{\delta}_2' \cos \beta - \dot{\delta}_2\beta' \sin \beta) \sin \beta \cos \beta \\
 &\quad + 2\Omega(I_\zeta^2 \sin^2 \beta + I_\eta^2 \cos^2 \beta)(\dot{\delta}_1' \cos \beta - \dot{\delta}_1\beta' \sin \beta + \dot{\delta}_2' \sin \beta + \dot{\delta}_2\beta' \cos \beta) \\
 q_\eta &= \Omega^2 I_\eta(\delta_1' + \delta_2\beta') - I_\eta(\ddot{\delta}_1' + \ddot{\delta}_2\beta') + 2\Omega I_\eta\dot{\beta} \cos \beta \\
 q_\zeta &= -\Omega^2 \rho e(x + u) + \rho e\ddot{u} - 2\rho e\Omega(-\dot{\delta}_1 \sin \beta + \dot{\delta}_2 \cos \beta) \\
 &\quad - \Omega^2 I_\zeta\delta_1\beta' + \Omega^2 I_\zeta\delta_2' + I_\zeta\ddot{\delta}_1\beta' - \ddot{I}_\zeta\ddot{\delta}_2' + 2\Omega I_\zeta\dot{\beta} \sin \beta .
 \end{aligned}$$

In the following, we eliminate terms in p_x which are dependent on displacement variables and their derivatives, since these lead to nonlinearities in subsequent analysis, and terms in all force and moment expressions which involve u and its derivatives and first derivatives of the remaining displacement variables. We also eliminate terms involving β' , since these terms arise when δ_1' and δ_2' are derivatives referred to the axes η and ξ rotating about the x axis. In the lumped parameter treatment, δ_1' and δ_2' can be considered to be derivatives with respect to locally fixed axes.

$$p_x = \Omega^2 \rho x$$

$$p_\eta = -\rho \ddot{\delta}_2 - \Omega^2 \rho \sin \beta (\cos \beta \delta_1 + \Omega^2 \rho (\cos^2 \beta \delta_2$$

$$- \Omega^2 \rho \sin \beta (2e \cos \beta + e_0) \phi + \Omega^2 \rho \cos \beta (e \cos \beta + e_0)$$

$$p_\xi = -\rho \ddot{\delta}_1 + \Omega^2 \rho (\sin^2 \beta \delta_1 - \Omega^2 \rho \sin \beta (\cos \beta \delta_2 - \rho e \ddot{\phi}$$

$$+ \Omega^2 \rho \left\{ e (\sin^2 \beta - \cos^2 \beta) - e_0 \cos \beta \right\} \phi - \Omega^2 \rho \sin \beta (e \cos \beta + e_0)$$

(B2)

$$q_x = -\rho e \ddot{\delta}_1 + \Omega^2 \rho e (\sin^2 \beta \delta_1 - \Omega^2 \rho e \sin \beta (\cos \beta \delta_2$$

$$- \Omega^2 \left\{ \rho e e_0 \cos \beta + (I_\xi - I_\eta) \cos 2\beta \right\} \phi - (I_\xi + I_\eta) \ddot{\phi}$$

$$- \Omega^2 \sin \beta \left\{ \rho e e_0 + (I_\xi - I_\eta) \cos \beta \right\}$$

$$q_\eta = \Omega^2 I_\eta \delta_1' - I_\eta \ddot{\delta}_1'$$

$$q_\xi = \Omega^2 I_\xi \delta_2' - I_\xi \ddot{\delta}_2' - \Omega^2 \rho e x$$

Now, if we consider the matrix equation

$$\{\hat{\Delta}\}_N = [F]_N \{\Delta\}_N \quad (B3)$$

where $\{\Delta\}$ is

$$[\Delta] = \left\{ \begin{array}{c} V_1 \\ M_1 \\ \delta_1 \\ \delta_1' \\ V_2 \\ M_2 \\ \delta_2 \\ \delta_2' \\ Q \\ \phi \end{array} \right\} \quad (B4)$$

and $[\Delta]_N$ refers to the value of these quantities at station N just outboard of the mass, and $[\hat{\Delta}]_N$ refers to the values just inboard of the mass, it follows that

$$\begin{aligned} \hat{V}_1^{(N)} &= V_1^{(N)} + p_\zeta^{(N)} l^{(N)} \\ &= V_1^{(N)} + \rho^{(N)} l^{(N)} (\omega^2 + \Omega^2 \sin^2 \beta) \delta_1^{(N)} - \rho^{(N)} l^{(N)} \Omega^2 \cos \beta (\sin \beta) \delta_2^{(N)} \\ &\quad + \rho^{(N)} l^{(N)} \left[e^{(N)} (\omega^2 + (\sin^2 \beta - \cos^2 \beta) \Omega^2) + e_o \Omega^2 \cos \beta \right] \phi^{(N)} \\ &\quad - \rho^{(N)} l^{(N)} \Omega^2 \sin \beta (e_o^{(N)} + e^{(N)} \cos \beta) \\ \hat{M}_1^{(N)} &= M_1^{(N)} + q_\eta^{(N)} l^{(N)} - p_x^{(N)} l^{(N)} \delta_1^{(N)} \\ &= M_1^{(N)} - \rho^{(N)} l^{(N)} \Omega^2 x^{(N)} \delta_1^{(N)} + I_\eta^{(N)} l^{(N)} (\omega^2 + \Omega^2) \delta_1'^{(N)} \\ \hat{\delta}_1'^{(N)} &= \delta_1'^{(N)} \\ \hat{\delta}_1^{(N)} &= \delta_1^{(N)} \end{aligned} \quad (B5)$$

$$\begin{aligned}
\hat{V}_2^{(N)} &= V_2^{(N)} + p_\eta^{(N)} l^{(N)} \\
&= +V_2^{(N)} - \rho^{(N)} l^{(N)} \Omega^2 \sin \beta (\cos \beta) \delta_1^{(N)} \\
&+ \rho^{(N)} l^{(N)} (\omega^2 + \Omega^2 \cos^2 \beta) \delta_2^{(N)} \\
&- \rho^{(N)} l^{(N)} \Omega^2 \sin \beta (e^{(N)}_2 \cos \beta + e_o^{(N)}) \phi^{(N)} \\
&+ \rho^{(N)} l^{(N)} \Omega^2 \cos \beta (e_o^{(N)} + e^{(N)} \cos \beta)
\end{aligned}$$

$$\begin{aligned}
\hat{M}_2^{(N)} &= M_2^{(N)} + q_\zeta^{(N)} l^{(N)} - p_x^{(N)} l^{(N)} \delta_2^{(N)} \\
&= M_2^{(N)} - \rho^{(N)} l^{(N)} x^{(N)} \Omega^2 \delta_2^{(N)} - \rho^{(N)} l^{(N)} x^{(N)} e^{(N)} \Omega^2 + I_\zeta^{(N)} l^{(N)} (\omega^2 + \Omega^2) \delta_2^{(N)}
\end{aligned}$$

$$\hat{\delta}_2^{(N)} = \delta_2^{(N)} \quad (B5)$$

$$\hat{\delta}_2^{(N)} = \delta_2^{(N)}$$

$$\begin{aligned}
\hat{Q}^{(N)} &= Q^{(N)} + q_x^{(N)} l^{(N)} \\
&= \rho^{(N)} l^{(N)} e^{(N)} (\omega^2 + \Omega^2 \sin^2 \beta) \delta_1^{(N)} \\
&- \rho^{(N)} l^{(N)} e^{(N)} \Omega^2 \cos \beta (\sin \beta) \delta_2^{(N)} + Q^{(N)} \\
&+ \left[(I_\eta + I_\zeta)^{(N)} l^{(N)} \omega^2 + (I_\eta - I_\zeta)^{(N)} (\cos^2 \beta - \sin^2 \beta) l^{(N)} \Omega^2 \right. \\
&- \left. \rho^{(N)} e^{(N)} l^{(N)} e_o^{(N)} \Omega^2 \cos \beta \right] \phi^{(N)} \\
&(I_\eta - I_\zeta)^{(N)} l^{(N)} \Omega^2 \sin \beta \cos \beta - \rho^{(N)} l^{(N)} e^{(N)} e_o^{(N)} \Omega^2 \sin \beta
\end{aligned}$$

$$\hat{\phi}^{(N)} = \phi^{(N)}$$

APPENDIX C

DEFORMATION OF A BLADE SEGMENT

Consider a segment of a weightless beam for which the values of the moment, torque, shear, and tension at a station N are given as $M_1^{(N)}$, $M_2^{(N)}$, $Q^{(N)}$, $V_1^{(N)}$, $V_2^{(N)}$ and $T^{(N)}$. Then moments and torques at other points along the segment are

$$\begin{aligned} M_1 &= M_1^{(N)} + V_1^{(N)}s + T^{(N)}\delta_1 U^{(N)}\phi \\ M_2 &= M_2^{(N)} + V_2^{(N)}s + T^{(N)}\delta_2 + W^{(N)}\phi \\ Q &= Q^{(N)} + U^{(N)}\delta_1' \end{aligned} \quad (C1)$$

where $U^{(N)}$ and $W^{(N)}$ are the contributions of the centrifugal force coupling as explained in Appendix D, s is the longitudinal coordinate measured from station N toward the root, and primes denote differentiation with respect to s . These same quantities in terms of δ_1 and δ_2 for a twisted blade are

$$\begin{aligned} M_1 &= EI_1 \left[\delta_1'' + 2\beta'\delta_2' + \beta''\delta_2 - (\beta')^2\delta_1 \right] \\ M_2 &= EI_2 \left[\delta_2'' - 2\beta'\delta_1' - \beta''\delta_1 - (\beta')^2\delta_2 \right] - Te_A - EB_2\beta'\phi' \\ Q &= - \left[GJ_e + Tk_A^2 + EB_1(\beta')^2 \right] \phi' - Tk_A^2\beta' \\ &\quad + EB_2\beta' \left[\delta_2'' - 2\beta'\delta_1' - \beta''\delta_1 - (\beta')^2\delta_2 \right] \end{aligned} \quad (C2)$$

For a straight segment Eqs. (C2) reduce to

$$\begin{aligned} M_1 &= EI_1\delta_1'' \\ M_2 &= EI_2\delta_2'' - Te_A - EB_2\beta'\phi' \\ Q &= - \left[GJ_e + Tk_A^2 + EB_1(\beta')^2 \right] \phi' - Tk_A^2\beta' + EB_2(\beta')\delta_2'' \end{aligned} \quad (C3)$$

Eliminating steady-state terms and combining Eqs.(C1) and (C3),

$$\begin{aligned}
 \delta_1'' - a_1\delta_1 - a_2\phi' &= b_1s + b_2 \\
 \delta_2'' - a_3\delta_2 - a_4\phi' - a_5\phi &= b_3s + b_4 \\
 a_6\delta_1' - a_7\delta_2'' + a_8\phi' &= -b_5
 \end{aligned} \tag{C4}$$

where

$$\begin{aligned}
 a_1 &= \frac{T^{(N)}}{EI_1} & b_1 &= \frac{V_1^{(N)}}{EI_1} \\
 a_2 &= \frac{U^{(N)}}{EI_1} & b_2 &= \frac{M_1^{(N)}}{EI_1} \\
 a_3 &= \frac{T^{(N)}}{EI_2} & b_3 &= \frac{V_2^{(N)}}{EI_2} \\
 a_4 &= \frac{EB_2\beta'}{EI_2} & b_4 &= \frac{M_2^{(N)}}{EI_2} \\
 a_5 &= -\frac{W^{(N)}}{EI_2} & b_5 &= Q^{(N)} \\
 a_6 &= U^{(N)} \\
 a_7 &= EB_2\beta' \\
 a_8 &= A^{(N)} = GJ_e + Tk_A^2 + EB_1(\beta')^2
 \end{aligned}$$

These equations may be solved as they stand; however, considerable simplification can be achieved at a modest sacrifice in accuracy by replacing the term $a_5\phi$ by $a_5\phi^{(N)}$. This modifies the second of Eqs. (C4) to read

$$\delta_2'' - a_3\delta_2 - a_4\phi' = b_3s + b_6 \tag{C5}$$

where

$$b_6 = \frac{W^{(N)}}{EI_2} \phi^{(N)} + \frac{M_2^{(N)}}{EI_2} .$$

The characteristic equation for the new set becomes

$$f_0 p^4 + f_1 p^2 + f_2 = 0 \quad (c6)$$

where

$$f_0 = (a_8 - a_4 a_7)$$

$$f_1 = a_2 a_6 - a_8 (a_1 + a_3) + a_1 a_4 a_7$$

$$f_2 = a_1 a_3 a_8 - a_2 a_3 a_6 .$$

The roots of this equation are then

$$p_{1,2}^2 = -\frac{f_1}{2f_0} \pm \frac{1}{f_0} \sqrt{\left(\frac{f_1}{2}\right)^2 - f_0 f_2} . \quad (c7)$$

When the solution is carried out, with the elements of $\{\Delta\}^{(N)}$ as initial values, and s is taken equal to 1, the following form for the solution results

$$\begin{aligned} \delta_1^{(N+1)} &= \sum_{j=1}^{10} E_{3j} \Delta_j \\ \delta_1^{(N+1)} &= \sum_{j=1}^{10} E_{4j} \Delta_j \\ \delta_2^{(N+1)} &= \sum_{j=1}^{10} E_{7j} \Delta_j \end{aligned} \quad (c8)$$

$$\begin{aligned}
\delta_2^{(N+1)} &= \sum_{j=1}^{10} E_{8j} \Delta_j \\
\phi^{(N+1)} &= \sum_{j=1}^{10} E_{10j} \Delta_j
\end{aligned} \tag{C8}$$

where the E_{ij} are presented in Eq. (2.6) in the body of the report and Δ_j are the elements of $\{\Delta\}^{(N)}$ given in Eq. (2.1).

The remaining E_{ij} elements are found from the following equations which apply across each bay

$$\begin{aligned}
V_1^{(N+1)} &= V_1^{(N)} \\
M_1^{(N+1)} &= M_1^{(N)} + V_1^{(N)} l \\
V_2^{(N+1)} &= V_2^{(N)} \\
M_2^{(N+1)} &= M_2^{(N)} + V_2^{(N)} l \\
Q^{(N+1)} &= Q^{(N)}
\end{aligned} \tag{C9}$$

It should be noted that the bending moment and torque quantities in Eqs. (C9) by definition do not include the contributions of the centrifugal force displaced to the elastic axis and of centrifugal coupling. These contributions are introduced separately through satisfaction of Eqs. (C1) in the solution for the deformation variables.

APPENDIX D

CENTRIFUGAL FORCE COUPLING

As shown in Ref. 2, there is a type of coupling between bending and torsion associated with the presence of centrifugal forces. Explicit consideration must be given to the derivation of the terms associated with this coupling.

If x_1 is used to denote the station where centrifugal force is acting and x the station where bending moment is measured, the components of bending moment associated with offset of mass center from the elastic axis of the rotating blade may be written as follows:

$$\begin{aligned}
 M_1 &= -\cos(\beta+\phi) \int_x^R \Omega^2 \rho_1 x_1 e_1 \sin(\beta_1+\phi_1) dx_1 \\
 &\quad + \sin(\beta+\phi) \int_x^R \Omega^2 \rho_1 x_1 e_1 \cos(\beta_1+\phi_1) dx_1 \\
 M_2 &= -\sin(\beta+\phi) \int_x^R \Omega^2 \rho_1 x_1 e_1 \sin(\beta_1+\phi_1) dx_1 \\
 &\quad - \cos(\beta+\phi) \int_x^R \Omega^2 \rho_1 x_1 e_1 \cos(\beta_1+\phi_1) dx_1
 \end{aligned} \tag{D1}$$

where subscript 1 refers to values at x_1 .

Assuming ϕ to be a small angle and eliminating higher order terms, Eqs. (D1) become,

$$\begin{aligned}
 M_1 &= -\cos \beta \int_x^R \Omega^2 \rho_1 x_1 e_1 \sin \beta_1 dx_1 + \phi \sin \beta \int_x^R \Omega^2 \rho_1 x_1 e_1 \sin \beta_1 dx_1 \\
 &\quad - \cos \beta \int_x^R \Omega^2 \rho_1 x_1 e_1 \phi_1 \cos \beta_1 dx_1 \\
 &\quad + \sin \beta \int_x^R \Omega^2 \rho_1 x_1 e_1 \cos \beta_1 dx_1 + \phi \cos \beta \int_x^R \Omega^2 \rho_1 x_1 e_1 \cos \beta_1 dx_1 \\
 &\quad - \sin \beta \int_x^R \Omega^2 \rho_1 x_1 e_1 \phi_1 \sin \beta_1 dx_1
 \end{aligned} \tag{D2}$$

$$\begin{aligned}
M_2 = & - \sin \beta \int_x^R \Omega^2 \rho_1 x_1 e_1 \sin \beta_1 dx_1 - \phi \cos \beta \int_x^R \Omega^2 \rho_1 x_1 e_1 \sin \beta_1 dx_1 \\
& - \sin \beta \int_x^R \Omega^2 \rho_1 x_1 e_1 \phi_1 \cos \beta_1 dx_1 \\
& - \cos \beta \int_x^R \Omega^2 \rho_1 x_1 e_1 \cos \beta_1 dx_1 + \phi \sin \beta \int_x^R \Omega^2 \rho_1 x_1 e_1 \cos \beta_1 dx_1 \\
& + \cos \beta \int_x^R \Omega^2 \rho_1 x_1 e_1 \phi_1 \sin \beta_1 dx_1
\end{aligned} \tag{D2}$$

In each case, the first and fourth terms represent steady-state moments. An examination of Appendix B shows that the term $-\Omega^2 \rho e x$ in q_ζ will give rise to these moments. They are taken into account through the element d_6 in the $\{d\}$ matrix.

The third and sixth terms in each component represent the effect of torsional displacement of the blade mass on bending about the torsionally undisplaced positions of the η and ξ axes in the M_1 and M_2 components respectively. This effect can be taken into account by an appropriate modification of the $[F]$ matrix, incorporating a change in bending moment across each mass given by

$$\Delta M_1 = - \Omega^2 \rho l x e \phi \tag{D3}$$

yielding the element

$$F_{210} = - \Omega^2 \rho l x e \tag{D4}$$

The second and fifth terms represent the effect of centrifugal forces acting on the torsionally undisplaced masses between x and R on bending about the torsionally displaced η and ξ axes in the M_1 and M_2 components respectively. They must be taken into account in the development of the $[E]$ matrix. In terms of the lumped mass model, the contribution to the bending moments in the bay between the n th and $(n+1)$ th masses is

$$\begin{aligned}
M_1 &= \left(\sin \beta_n \sum_{i=1}^n \Omega^2 \ell_i \rho_i x_i e_i \sin \beta_i + \cos \beta_n \sum_{i=1}^n \Omega^2 \rho_i \ell_i x_i e_i \cos \beta_i \right) \phi \\
&= U^{(N)} \phi \\
M_2 &= \left(-\cos \beta_n \sum_{i=1}^n \Omega^2 \rho_i \ell_i x_i e_i \sin \beta_i + \sin \beta_n \sum_{i=1}^n \Omega^2 \rho_i \ell_i x_i e_i \cos \beta_i \right) \phi \\
&= W^{(N)} \phi
\end{aligned} \tag{D5}$$

There is correspondingly an effect of bending on torque. It is associated with the fact that with a bending slope δ_1' at station x the centrifugal force $\Omega^2 \rho_1 x_1 dx_1$ on an element dx_1 at station x_1 outboard of station x has a component $-\Omega^2 \rho_1 x_1 dx_1 \delta_1'$ normal to the η -axis in the plane of the cross section at station x . The moment arm of this force about the elastic axis is $e_1 \cos(\beta - \beta_1)$, so that the contribution to the torque from this source may be written,

$$\begin{aligned}
Q &= -\delta_1' \int_x^R \Omega^2 \rho_1 x_1 e_1 \cos(\beta - \beta_1) dx_1 \\
&= - \left(\sin \beta \int_x^R \Omega^2 \rho_1 x_1 e_1 \sin \beta_1 dx_1 + \cos \beta \int_x^R \Omega^2 \rho_1 x_1 e_1 \cos \beta_1 dx_1 \right) \delta_1' \tag{D6}
\end{aligned}$$

Applying this result to the lumped mass model, the contribution to the torque in the bay between the n th and $(n+1)$ th masses is

$$Q = - \left(\sin \beta_n \sum_{i=1}^n \Omega^2 \rho_i \ell_i x_i e_i \sin \beta_i + \cos \beta_n \sum_{i=1}^n \Omega^2 \rho_i \ell_i x_i e_i \cos \beta_i \right) \delta_1' \tag{D7}$$

and is taken into account in the development of the $[E]$ matrix in Appendix C.

REFERENCES

1. Isakson, G., and Eisley, J. G.: Natural Frequencies in Bending of Twisted Rotating Blades. NASA TN D-371, March, 1960.
2. Houbolt, J. C., and Brooks, G. W.: Differential Equations of Motion for Combined Flapwise Bending, Chordwise Bending, and Torsion of Twisted Nonuniform Rotor Blades. NACA Rept. 1346. (Supersedes NACA TN 3905.)
3. Targoff, W.: The Bending Vibrations of a Twisted Rotating Beam. Proc. Third Midwestern Conf. on Solid Mech. (Ann Arbor, Mich., 1956), 1957, pp. 177-194. (Also WADC Tech. Rept. 56-27.)
4. Brady, W. G., and Targoff, W. P.: Uncoupled Torsional Vibrations of a Thin, Twisted, Rotating Beam. WADC Tech. Rept. 56-501, June, 1957. (ASTIA Document Nr. AD 130786.)
5. Niedenfuhr, F. W.: On the Possibility of Aeroelastic Reversal of Propeller Blades. Jour. Aero. Sciences, Vol. 22, No. 6, June, 1955, pp. 438-440.
6. Bogdanoff, J. L., and Horner, J. T.: Torsional Vibration of Rotating Twisted Bars. Jour. Aero. Sciences, Vol. 23, No. 4, April, 1956, pp. 303-305.
7. Bogdanoff, J. L.: Influence of Secondary Inertia Terms on Natural Frequencies of Rotating Beams. Jour. App. Mech., Vol. 22, No. 4, December, 1955, pp. 587-591.
8. Doolin, Brian F.: The Application of Matrix Methods to Coordinate Transformations Occurring in Systems Studies Involving Large Motions of Aircraft. NACA TN 3968, May, 1957.

"The aeronautical and space activities of the United States shall be conducted so as to contribute . . . to the expansion of human knowledge of phenomena in the atmosphere and space. The Administration shall provide for the widest practicable and appropriate dissemination of information concerning its activities and the results thereof."

—NATIONAL AERONAUTICS AND SPACE ACT OF 1958

NASA SCIENTIFIC AND TECHNICAL PUBLICATIONS

TECHNICAL REPORTS: Scientific and technical information considered important, complete, and a lasting contribution to existing knowledge.

TECHNICAL NOTES: Information less broad in scope but nevertheless of importance as a contribution to existing knowledge.

TECHNICAL MEMORANDUMS: Information receiving limited distribution because of preliminary data, security classification, or other reasons.

CONTRACTOR REPORTS: Technical information generated in connection with a NASA contract or grant and released under NASA auspices.

TECHNICAL TRANSLATIONS: Information published in a foreign language considered to merit NASA distribution in English.

TECHNICAL REPRINTS: Information derived from NASA activities and initially published in the form of journal articles.

SPECIAL PUBLICATIONS: Information derived from or of value to NASA activities but not necessarily reporting the results of individual NASA-programmed scientific efforts. Publications include conference proceedings, monographs, data compilations, handbooks, sourcebooks, and special bibliographies.

Details on the availability of these publications may be obtained from:

SCIENTIFIC AND TECHNICAL INFORMATION DIVISION
NATIONAL AERONAUTICS AND SPACE ADMINISTRATION

Washington, D.C. 20546